Geospatial organization of fluvial landforms in a gravel–cobble river: beyond the riffle–pool couplet

J.R. Wyrick and G.B. Pasternack*

University of California, Davis, One Shields Drive, Davis, CA 95616, USA

* Corresponding author. Tel.: + 1 530-302-5658; Fax: + 1 530-752-5262;
E-mail: gpast@ucdavis.edu.

Abstract

Morphological units (MU) are landforms with distinct local form–process associations at ~ 1-10 channel widths scale that may be the fundamental building blocks describing the geomorphic structure of a river. Past research has disproportionately focused on the two MUs of pool and riffle, conjecturing that they are the central linked couplet in the process–form association. The goal of this study was to delineate and map spatially explicit fluvial landforms in two-dimensional planview within a gravel–cobble bed river using two-dimensional hydrodynamic delineation and then to statistically examine MU geospatial patterns for indicators of deterministic geomorphic control. This procedure is not discharge-dependent like mesohabitat methods, but gets at the geometry of underlying landforms. Statistical testing confirmed that eight delineated in-channel MU types comprise a complex and diverse channel morphology in which pools and riffles are not directly coupled. Specifically, gravel–cobble river channels (1) exhibit nonrandom spatial organization of their longitudinally and laterally variable landform morphology; (2) consist of a variety of MU types, not just pools and riffles; and (3) show distinct MU collocations and avoidances, with riffles linked to chutes and runs, while pools are linked to slackwaters and glides. Planview MU delineation with two-dimensional hydrodynamic modeling provides a 'bottom-up' approach to understanding and linking channel morphology with ecosystem services and geomorphic processes and is being used to guide river management and rehabilitation strategies.

Keywords: morphological unit; channel unit; riffles; pools; river landforms

1. Introduction

A river channel is a complex configuration of morphologies, ranging from the dendritic drainage networks at the catchment scale to cobble clusters at the centimeter scale. The spatial patterns of rivers have long intrigued fluvial scientists, and much literature is available that is focused on the attempt to define and classify these patterns at all spatial and temporal scales. For the research presented herein, the landforms within a long channel segment will be analyzed at the morphological unit scale (~ 1-10 channel widths, W).

The mapping of river morphology at the 1-10 W scale is common practice for researchers studying fluvial systems and is well reported in the literature. Several terms exist for discernible units at this scale, such as *channel unit* (e.g., Grant et al., 1990; Bisson et al., 1996), *channel geomorphic unit* (e.g., Hawkins et al., 1993), *morphological unit* (e.g., Wadeson, 1994), and *physical biotope* (e.g., Newson and Newson, 2000). The term *morphological unit* (MU) is used in this study in order to not be confined to just the channel as well as to avoid imposing any habitat requirement.

A review of previous landform studies shows that MUs are typically identified but then their spatial organization is mostly ignored, with the focus instead on correlations between individual MU types and channel gradient (Halwas and Church, 2002), how habitat varies with discharge (e.g., Hauer et al., 2009) or time (e.g., Madej, 2001; Klaar et al., 2009), their associated hydraulics (e.g., Wadeson and Rowntree, 1998), or using the units as a basis for segregating biologic data (e.g., Zimmer and Power, 2006; Schwartz and Herricks, 2008). Among previous studies that did analyze the spatial organization of MUs, the most common metric reported is that of one-dimensional longitudinal spacing between riffles and pools (e.g., Keller and Melhorn, 1978; Gregory et al., 1994), which are also usually coupled into a single ‘unit’ (e.g., Thompson, 1986). However, one-dimensional studies ignore lateral variability in channel morphology, an aspect that is key to diverse hydraulics and habitat. A few studies have also reported abundance percentages and streamwise sequences of unit-to-unit transitions (e.g., Grant et al., 1990; Borsanyi et al., 2004).

Significant differences in channel delineation exist between biologists and geomorphologists. When delineating gravel–cobble channels into habitats at the 1-10 W scale for biologic purposes, a large catalog of unit types and descriptions exists (e.g., Maddock, 1999; Newson and Newson, 2000). However, when delineating channels into MUs for geomorphic purposes, the catalog of commonly published types primarily reduces to pools and riffles, which are the elevational end members (e.g., O’Neill and Abrahams, 1984; Thompson, 1986). The spatial patterns of other MUs such as runs, chutes, and glides might be just as important for assessing the channel complexity and habitat potential but are rarely investigated (e.g., Grant et al., 1990; Moir and Pasternack, 2008). This study delineated eight distinct MUs and evaluated the spatial organization of all of them with respect to the channel segment and to each other.

The spatial heterogeneity of fluvial landforms is important to ascertain because it can be an indicator of the ‘health’ of a river. High complexity of landforms generally equates to high diversity of hydraulics and thus high biodiversity across all ecologic lifestages (e.g., Frissell et al., 1986; Newson and Newson, 2000), although Newson and Large (2006) do caution against a pure correlation of only equating geodiversity to biodiversity from a habitat management viewpoint. However, geodiversity in fluvial landforms does at least set a framework for habitat protection and conservation (Gray, 2004), and thus evaluation of the channel at the 1-10 W scale is key to assessing the physical habitat (Maddock, 1999). As an example of this correlation, Reid et al. (2008) showed that poor habitat conditions of river reaches are generally associated with a low diversity of MUs. Channel complexity should ideally be described by the composition and the configuration of MUs, where a highly complex channel would exhibit statistically nonrandom patterns for each metric, with examples of such tests developed and provided herein.

The debate over the appropriate number and definitions of fluvial landforms is far from over, and there is especially a lack of published studies that analyze landforms within a planview geospatial context. The goal of this study was thus to delineate and map fluvial landforms of a gravel–cobble bed river as objectively as possible aided with two-dimensional (2D) hydrodynamic modeling and then to statistically examine geospatial patterns for indicators of systematic geomorphic control. The results presented herein illustrate how complex and diverse a channel's morphology can be.

2. Study site

The Yuba River is a tributary of the Feather River in north-central California, USA, that drains 3480 km^2 of the western Sierra Nevada range (Fig. 1). The watershed has a history of hydraulic mining that is the source of the present alluvium. Englebright Dam was built in 1940 to trap nearly all sediment and thereby promote downstream geomorphic recovery, which continues to proceed more than 70 years later (Carley et al., 2012). Daguerre Point Dam (DPD) is an 8-m high irrigation diversion structure located at river kilometre (RKM) 17.8 that creates a slope break and partial sediment barrier. Instantaneous stage-discharge has been continuously recorded at the USGS gages at Smartsville near Englebright Dam (#11418000), at Marysville near the mouth (#11421000) (Fig. 1), and on the regulated tributary Deer Creek (#11418500). Base flow typically occurs during the late fall season when Chinook (*Oncorhynchus tshawytscha*) adults spawn.

The 37.1-km river segment between Englebright Dam and the Feather River confluence is defined as the lower Yuba River (LYR). The LYR is a single-thread channel (~ 20 emergent bars/islands at bankfull) with low sinuosity, high width-to-depth ratio, and slight to no entrenchment. The geomorphically determined bankfull discharge was estimated as 141.6 m^3/s, which has ~ 82% annual exceedance probability. The river corridor is confined in a steep-walled bedrock canyon for the upper 3.1 RKM, then transitions first into a wider bedrock valley with some meandering through Timbuctoo Bend (RKM 28.3-34.0; Fig. 1), then into a wide, alluvial valley downstream to the mouth. Hydraulic mining sediment was used to train the active river corridor in the wide lowlands to isolate it from the ~ 4,000 ha Yuba Goldfields. Riverbed thalweg elevations range from ~ 9 to 88 m above mean sea level (NAVD88 datum), with a mean bed slope of 0.185%. The segment-scale mean diameter of the channel sediment is 97 mm (i.e., small cobble). In the bedrock canyon just below Englebright Dam, the mean wetted width at base-flow discharge is 36.4 m. The remainder of the base-flow channel upstream of DPD widens to a mean wetted width of 64.6 m, and then the channel below DPD narrows slightly to a mean wetted width of 56.4 m. At bankfull, the mean widths are 51.4, 99.4, and 98.4 m, respectively, for those same regions. As a comparison to other rivers, the LYR is classified as a C3 channel by the Stream Type classification method (Rosgen, 1996) and as transitional between straight and meandering by the flow instability method (Parker, 1976). Existing literature with more information about the hydrogeomorphic conditions of the LYR includes Pasternack (2008), Moir and Pasternack (2008, 2010), James et al. (2009), Sawyer et al. (2010), White et al. (2010), Wyrick and Pasternack (2012), and Abu-Aly et al. (2013).

3. Physical data collection

3.1. Topographic and bathymetric mapping

River corridor topography and bathymetry were collected for the high resolution digital elevation model (DEM) using a combination of ground-based, boat-based, and remote sensing methods in accordance with a predesigned protocol (Pasternack, 2009; Carley et al., 2012). Different regions were mapped at different times between 2006 and 2009 as funding permitted. Each survey method involved its own internal performance tests, such as backsight checks, GPS root mean square values, and comparison of airborne Light Detection and Ranging (LiDAR) observations to ground-based observations on flat, smooth roads. The only gap in the DEM is the Narrows Reach (RKM ~ 34-36), which contains unwadable, unboatable, air bubble-prolific, and therefore unsurveyable rapids. On 21 September 2008, Aero-Metric, Inc. (Seattle, WA) acquired LiDAR bare earth elevations of the river corridor during a constant low flow typical of the period when hydro facility maintenance takes place: 24.4 m^3/s between Englebright Dam and DPD and 17.6 m^3/s below DPD where irrigation diversions occur. A professional hydrography firm (Environmental Data Solutions, San Rafael, CA) collected bathymetric points along longitudinal and cross-channel lines, meeting class 1 standard (± 0.5 feet vertical accuracy). Because some areas were inaccessible by boat or were easier to map by wading, ground crews surveyed sections of the channel with either a robotic total station (Leica TPS1200) or a real-time kinetic (RTK) GPS (Trimble R7). All of the different surveys were tied together with a common array of benchmarks and vertical adjustment to a common vertical datum (NAVD 88). The resulting reach-averaged topographic point density ranged from 28 to 60 and from 11 to 554 points/100 m^2 within and beyond the 24.92 m^3/s base-flow domain, respectively. Low densities are associated with ground-based surveys.

Quality assurance and quality control procedures were applied to the field data, and then a DEM was produced. Data from every different survey was compared against every other method at overlaps to assess uncertainty. For example, a comparison of boat-based water surface elevations versus those from ground-based RTK GPS at the adjacent water's edge yielded observed vertical differences of 75% of test points within 3 cm, 91% within 6 cm, and 99% within 15 cm. After accounting for data quality, acceptable points were visualized in ArcGIS software (ESRI, Redlands, CA) and further edited on a spatial basis to remove obvious errors. In narrow backwater channels and along banks that contained obvious interpolation errors, hydro-enforced breaklines and regular breaklines were created to better represent landform features. Additionally, some bathymetric areas that contained very few points because of obstructions and other problematic features were artificially augmented, so that channel characteristics were maintained. A TIN-based DEM was produced as the native terrain model from which derivative rasters and contours were produced as needed.

3.2. Two-dimensional hydrodynamic model

The surface-water modeling system (Aquaveo, LLC, Provo, UT) and sedimentation and river hydraulics–two-dimensional (SRH-2D; Lai, 2008) were used to produce 2D hydrodynamic models of the LYR according to the procedures of Pasternack (2011). This model has a 2D finite-volume solver for depth-averaged shallow water equations to estimate depth and velocity at each computational node. Details about the LYR 2D model are in Barker (2011), Abu-Aly et al. (2013), and Pasternack et al. (2013). Because the LYR 2D model is a local management tool, it was built in English units, so reported values herein using SI units may seem unusual. This study only used simulations for base flows of 15.01 and 24.92 m^3/s, as well as the geomorphically determined bankfull flow of 141.58 m^3/s. The typical internodal spacing of each computational mesh for this range of flows was either 0.91 or 1.5 m. Input discharge was obtained from the USGS stations listed in section 2, accounting for agricultural diversion at DPD. Water surface elevations at the exit of each model domain for base flow were directly surveyed, while those for bankfull discharges were either surveyed or obtained from rating curves made with automated water-level loggers.

Boundary roughness was partially addressed by creating a highly detailed DEM, with unresolved roughness addressed by using a constant Manning's roughness value (*n*) for unvegetated terrain in each reach. Past site-scale 2D model studies on the LYR used an *n* of 0.043 for the unvegetated, gravel–cobble riverbed (Moir and Pasternack, 2008; Sawyer et al., 2010). For the long model domains in this study, an evaluation of observed and modeled water surface elevations at a range of in-channel flows up to bankfull found that an *n* of 0.04 was best downstream of DPD, an *n* of 0.032 best for the bedrock canyon below Englebright Dam, and an *n* of 0.03 best for the valley-confined Timbuctoo Bend (Pasternack et al., 2013). Based on LiDAR mapping of the vegetation canopy, the area of vegetation at base flow was < 4% and likely consisted of overhanging canopy, so vegetation was not quantified in boundary roughness. At bankfull discharge, indicators of boundary roughness showed no difference from that at base flow, so the same unvegetated *n* values were used.

The suitability of the constant roughness values (among other model aspects) was carefully tested by model validation using independent data spanning an order of magnitude of discharge (~ 14 to 170 m^3/s). Full model validation details were reported in Barker (2011). Mass conservation between specified input flow and computed output flows was within 1%. Water surface elevation performance can be evaluated relative to a river's mean substrate size because grain-scale topographic variation and water surface fluctuations limit WSE observation accuracy. For the LYR, the mean substrate size was ~ 10 cm (Wyrick and Pasternack, 2012). The mean signed vertical deviation for 197 observations at 24.92 m^3/s was -1.8 mm. For unsigned deviations (i.e., absolute values), 27% were within 3.1 cm vertical, 49% of deviations within 7.62 cm, 70% within 15.25 cm, and 94% within 30.5 cm. From cross-sectional surveys yielding 199 observations, predicted versus observed depths yielded a good coefficient of determination (r^2) of 0.66. Using Lagrangian tracking of an RTK GPS on a floating kayak, surface velocity magnitude was measured by Barker (2011) at 5780 locations, yielding a very good predicted versus observed r^2 of 0.79. Median unsigned velocity magnitude error was 16%, which is less than commonly reported. Using Lagrangian tracking of an RTK GPS on a floating kayak, velocity direction was also tested at those 5780 points, yielding a predicted versus observed r^2 of 0.80. This parameter is not commonly tested, but likely should be for 2D models. Median direction error was 4%, with 61% of deviations within 5° and 86% of deviations within 10°. Overall, the LYR 2D model met or exceeded all common standards of 2D model performance.

4. Morphological unit map

To identify and delineate the MUs, base-flow hydraulics were used to infer underlying channel morphology. Specific geomorphic landforms were assumed to exhibit discrete combinations of depth and velocity at a representative base flow. A complete and contiguous map of MUs was obtained from two inputs: (i) spatial grids of depth and velocity at a low steady discharge (when topography is the primary control on hydraulics) estimated using a 2D hydrodynamic model, and (ii) an expert-specified MU classification scheme using depth and velocity threshold values. With these inputs, all raster pixels were objectively classified into an MU type with a GIS-based algorithm, and then coherent MUs were identified as adjacent aggregates of individually classified points.

The channel bed within the base-flow wetted area was delineated into contiguous polygons of coherent landforms using a six-step procedure (Fig. 2) following the methodology presented in more detail in Pasternack (2011) and Wyrick and Pasternack (2012). First, detailed topographic and bathymetric data of the LYR were obtained and a DEM was produced (section 3.1). Second, expert judgment and local knowledge (guided from observations during data collection) were used to predetermine the number and nomenclature of MU types to be mapped, and then the range of each hydraulic variable was estimated for each MU type. Hydraulic thresholds were codified into an algorithm for classifying individual raster cells. Third, an appropriate low flow regime was identified at which to delineate MUs. Fourth, a 2D hydrodynamic model was developed, run, and validated for MU delineation at the LYR base flow (section 3.2). Fifth, rasters of the key delineation variables (i.e., depth and velocity) were created consistent with the resolution of the 2D model. Sixth, the objective MU delineation algorithm was applied to obtain a preliminary MU map. Lastly, the MU map was reviewed and evaluated by a diverse team of LYR experts to determine whether the MU types and hydraulic thresholds used in the process yielded meaningful patterns.

4.1. Base flow selection

For the LYR, controllable flows are set by flow schedules in the Lower Yuba Accord Fisheries Agreement (2007), but often enough flow occurs to operate above minimum requirements. A typical base-flow regime consists of ~ 24.92 m^3/s (~ 0.18 times bankfull) out of Englebright Dam, no discharge out of either of the two tributaries (whose outflows are normally 0-0.142 m^3/s when the LYR is at base flow), and a societal withdrawal of 9.91 m^3/s of water at Daguerre Point Dam (DPD), yielding a Marysville gage flow of 15.01 m^3/s. Because of this withdrawal, a paired discharge regime is appropriate to use here (i.e., combining model results for 24.92 m^3/s above DPD with 15.01 m^3/s results below DPD) for MU mapping to account for the diversion, instead of using a theoretical constant discharge for the whole river. The selected base-flow discharges are equivalent to ~ 75% daily exceedance probability.

The methodology of delineating MUs is robust enough that the resultant map is not sensitive to the selected base-flow discharge. When carefully analyzed for procedures and assumptions, virtually all landform mapping methods that exist today have a hydraulic dependency, including methods that use topographic longitudinal profiles. In the approach used in this study, experts establish which landforms are indicated by each range of depth and velocity at the selected discharge. Sensitivity analysis by Wyrick and Pasternack (2012) found that fixed hydraulic thresholds accurately reflect underlying topography for discharge variations within ~ ±15%. However, there is no sensitivity limit when thresholds are adjusted by experts to the modeled discharge. Thus, reliance on hydraulics does not mean that the methodology only captures discharge-dependent habitats; it actually does get at underlying landforms.

4.2. MU names and definitions

Moir and Pasternack (2008) previously created a hand-drawn MU map for a 457-m-long site on the LYR at the apex of Timbuctoo Bend (Fig. 1) guided by field experience, a DEM, and hydraulic rasters. This MU map, despite its subjectivity, provided thoughtful expert opinion and thus was a useful guide in selecting hydraulic metrics for the full LYR segment. Building from their study, Pasternack (2008) made an incremental improvement by using objective depth and topographic indicators along with subjective velocity estimates to map the MUs in all of Timbuctoo Bend, including several additional MU types that were not used in the initial site by Moir and Pasternack (2008). Building on Pasternack (2008) and drawing on commonly accepted descriptions, the MUs were identified, defined, and delineated for this study (Table 1, wherein descriptions of depth and velocity refer to those that are created by the landforms during the base-flow discharge used for this analysis).

4.3. MU mapping process

The resultant hydraulic rasters (0.91 x 0.91 m^2) were used to delineate eight in-channel MUs based on quantitative thresholds of depth and velocity (Fig. 3) in ArcGIS. Initial threshold values were based on and manipulated from the MU maps of Moir and Pasternack (2008) and Pasternack (2008). The resulting trial pattern was overlain on National Agricultural Image Program (NAIP) imagery. A visual inspection of the imagery was made by a group of LYR biologists, engineers, and geomorphologists with extensive ground-based experience. Their assessments were used to determine if the trial MU pattern conceptually conformed to the kind of MU delineation that would be yielded solely by subjective expert geomorphological opinion. These deliberations were not used to check or evaluate exact boundaries, however, which are more precisely specified by the computer algorithm than by eye or GPS. An iterative process of consensus-based adjustment to MU names, definitions, and thresholds led to the final set of depth and velocity threshold values (Fig. 3).

5. Spatial pattern analysis methods

MU spatial organization was analyzed from a segment-scale perspective. Statistical comparisons were derived from evaluating the organization of each MU type against the others and incorporating them into a broader context of geomorphic concepts. Overall composition and organization comparisons of the LYR against other specific rivers require more applications of this new methodology. For this study, the analyses focused on the sizes of polygons of each MU type and the diversity of polygon sizes amongst all MUs, which then guide an analysis to determine the minimum size of an MU that is statistically relevant and readily identifiable in the field. The remaining spatial analyses then include duplicate analyses and discussions in which all delineated polygons were used versus using only those that satisfy the minimum size criteria. The spatial analyses investigated to characterize MU organization include longitudinal distributions, longitudinal spacings between individuals of a given MU type, nondirectional adjacency collocations and avoidances between MU types, and the lateral abundance and variability of MUs at any given cross section. The locations of MUs are also placed in context with such hydromorphic characteristics as water surface slope, base-flow wetted width, and bankfull width–depth ratios.

5.1. Abundance and diversity

Previous MU studies reported total number of unique unit types, but not all quantify the total number and spatial coverage of each unit type compared against the others. This metric is important for assessing whether one or a few types tend to dominate the channel. If MUs randomly occur, no MU type would dominate and any particular location would have equal probability of becoming any MU. The total areas of each MU would therefore be equal to 100/n%, where n is the number of MU types specific to that river segment. Note that no known deterministic mechanism yet exists to yield uniform MU abundance among types.

To calculate the abundance of each MU type in the LYR, the area of each individual MU was calculated in ArcGIS. Polygon areas were summed by MU type and divided by the total wetted area to determine percent coverage. Additionally, histograms of polygon area were plotted for each MU type and compared among types.

The Shannon Diversity Index is a common method utilized to quantify the spatial complexity and heterogeneity of habitat but has also been applied to MUs (Maddock et al., 2008). Assessments of diversity (*H*), evenness (*J*), and dominance (*D*) of the total MU areas were calculated with the following equations:

$$H = -\Sigma(p_i \times \ln p_i) \quad (1)$$

$$J = H/\ln(N) \quad (2)$$

$$D = \ln(N) - H \quad (3)$$

where p_i is the fraction of total wetted area of the *i*-th MU type, and *N* is the total number of MU types. For the eight MU types in the LYR, a fully diverse composition would exhibit equal areas of each type (i.e., p_i = 1/8 = 0.125), a diversity index of 2.079, an evenness of 1.0, and a dominance factor of 0.0.

5.2. Longitudinal distribution

An important question is whether MUs are spatially organized or randomly located along a river segment. Most scientists assume they are organized, but that needs to be quantified for 2D MUs. By definition, if they are randomly located, then any particular location would have equal probability of being any MU. When that is the case, then the type of statistical distribution that is present is called a uniform distribution. No known deterministic mechanism yet exists to yield a uniform MU longitudinal distribution. The presence of a uniform distribution is indicated by having a horizontal discrete probability distribution function (PDF) and a diagonal straight-line cumulative distribution function (CDF) when probability of occurrence is plotted against channel distance. In a CDF, deviations of the slope from a straight-line trajectory indicate a higher or lower occurrence in a region of channel relative to the uniform expectation, where a steeper slope would indicate a higher occurrence and a lower slope would indicate a lower occurrence. Plotting the longitudinal distribution of the MUs shows whether a particular MU type tends to cluster in some regions of the channel or not.

The longitudinal distributions herein were calculated as the percent area of each MU type among all cross sections. Using ArcGIS, the river valley centerline was automatically stationed and given perpendicular cross sections evenly every 6 m (~ 1/10 base-flow width) along the study segment. Cross sections were then buffered 3 m upstream and downstream to create rectangles that spanned the wetted width and contiguously covered the segment area (see Fig. 4 for an example). Within each rectangle, the areas of each MU type were calculated and converted to a percent of total MU type area, and those areas were assigned to the cross section at each rectangle's center. Longitudinal distributions are presented as both discrete and cumulative area functions.

5.3. Longitudinal spacing

A commonly accepted notion in fluvial geomorphology is that longitudinal pool-riffle spacing is ~ 5-7 channel widths (W), as first postulated by Leopold et al. (1964) and supported by subsequent studies (e.g., Keller, 1972; Richards, 1976; Gregory et al., 1994). However, Keller (1972) reported that even though the mean spacing within his observed rivers was 5-7 W, the modes tended to be less (~ 3-5 W), which may be the result of the channel not being fully developed. O’Neill and Abrahams (1984) also calculated a mean spacing between riffles and pools to be within the 5-7 W range, but with a mode of ~ 3 W, which depended on their tolerance value of what they defined as a bedform. Other studies have also measured distances between riffles and pools in alluvial and mountain streams and found closer groupings than traditional values (i.e., < 5 W). For example, Carling and Orr (2000) found that riffle crests developed about once every 3 W in an alluvial channel and Montgomery et al. (1995) described pool spacings of ~ 2-5 W that were forced by logjams within steep channels. In short, while the commonly expressed spacing value between riffles or pools is 5-7 W, this is clearly not a universal value and deviances from this spacing could provide some insight into the channel’s development.

Additionally, even though the spacings between successive units have received considerable attention in the literature, the focus has only been on riffles and pools. In fact, even though Grant et al. (1990) identified and mapped five different channel unit types and analyzed their spatial organization, they only reported longitudinal spacing values for pools because of this lack of other studies with which to compare. This study thus evaluated the longitudinal spacings of all MUs that are longitudinally discrete as a start to the scientific dialogue for other landforms.

In ArcGIS, the centroid of each MU polygon in the LYR was determined and located perpendicularly to the nearest point along the channel’s base-flow thalweg. The distances along the thalweg for adjacent points of like MUs were then calculated.

Spacing analyses were performed in only the streamwise dimension; therefore, laterally adjacent units of the same type were not counted as separate units. The example site in Fig. 5 shows two riffle transition units located on the same cross section but on opposite banks of the channel. For analysis purposes, these two units were located to the same thalweg point and therefore only counted as one 'unit' in the calculations. Additionally, noncontiguous assemblages of the same type that are separated by pixilation effects were lumped as one discrete unit. Therefore, some discretion had to be employed to manually exempt some of the units from calculations. Because of this manual exemption, the statistical analysis was not performed using only those MUs larger than the minimum size threshold. The distances were then normalized by the mean bankfull channel width, which is consistent with what Keller (1972) reported.

5.4. Adjacency

An underutilized approach to investigating morphological unit organization is the transition probability analysis method of Grant et al. (1990). This approach evaluates the frequency that each morphological unit is adjacent to every other unit and then compares that against the expectation associated with a random system. This approach should become more valuable now that detailed spatial data sets of fluvial landforms are becoming readily available. As a result of lack of use, no baseline yet exists as to what constitutes a 'normal' transition probability matrix, so an important first step is to apply the method for diverse natural and regulated streams and derive that. Another important metric is to identify particular preferential combinations that may represent complex morphological sites at a scale larger than the individual MUs.

Because the MU conceptualization used in this study involves lateral and longitudinal adjacency of units, a new procedure had to be developed to investigate transition probabilities, which in this analysis become nondirectional adjacency probabilities. The numbers of common boundaries between two separate MU types were counted. This type of adjacency is not necessarily one-to-one, however. That is, unit type A can be adjacent to X number of unit type B, while unit B can be adjacent to unit type A, a different Y number of times (Fig. 6). That happens because a single type A polygon can be long and touch multiple type B polygons, whereas in the inverse, all those B polygons are only touching the one type A polygon. In other words, this method does not count each individual transition, which would have to be one-to-one, but instead the metric that is counted is the number of unique adjacencies. As exemplified in Fig. 6, if three unit B polygons touch the same unit A polygon, then that counts as one adjacency for B to A, but in the inverse it counts as three adjacencies.

The way Grant et al. (1990) evaluated the likelihood that the transition probabilities were nonrandom was to randomly generate a sequence of units (with each unit equally likely to occur next in order of selection), calculate the random transition probabilities, and then compare the real transition probabilities to those. A possible issue with that method is that the outcome is sensitive to the specific sequence created at random. Conceivably, one could repeat the step several times and compare the real transition probabilities to the average of random ones. However, if one were to use a near infinite number of random sequences, then in the limit, by definition, the transition probabilities available for this analysis must converge on $1/N$, where N is the number of unit types, as an equal probability exists of any unit type randomly going to any of the other unit types. As a result, the natural tendency for adjacency to a unit type can be designated as a *collocation* (analogous to a *preference* for an organism, but recognizing that MUs are inanimate) on the basis of whether the percent of adjacencies to it are higher than 1/*N*. Similarly, a natural *avoidance* to adjacency occurs when the percent of adjacencies are lower than 1/*N*.

Utilizing tools in ArcGIS, the number of adjacencies in the LYR from one MU to another was counted. The process was repeated for all possible unit-to-unit combinations. The total number of adjacencies for a particular unit was summed, and the adjacencies for individual units were represented as percentages of that total. For the eight MU types in the LYR, the convergence value would be 1/8, or 12.5%. Each transition probability was then divided by this random percentage to create a matrix that deviates around a value of one. Adjacencies within 20% of this random value (i.e., 0.8-1.2) were considered *near-random*.

5.5. Lateral variability

Traditional research usually only considers spatial organization in one dimension, i.e., one MU per cross section (e.g., O'Neill and Abrahams, 1984; Grant et al., 1990). However, recent studies have shown that wide rivers exhibit natural lateral variability in form–process associations (e.g., Bisson et al., 1996; Borsanyi et al., 2004; Moir and Pasternack, 2008; Milan et al., 2010). To test this hypothesis on the LYR, the number of distinct MUs at each cross section were counted and compared.

This method utilized the same cross-sectional rectangles employed for the longitudinal analyses. For this approach, the total numbers of unique MU polygons were counted. If one polygon looped out of then back into the same rectangle, it only counted as one; however, if two separate polygons of the same unit type occurred within the same rectangle, it counted as two (examples of each of these are illustrated in Fig. 4). If a polygon spanned multiple cross-sectional rectangles, it would count separately for each cross section.

A wide channel section offers more space for more laterally adjacent MUs (and the inverse is thus true for narrow sections). So, the raw values could be skewed by abnormally wide or narrow cross sections. Therefore, results were normalized by the mean base-flow width by dividing the number of MUs at each cross section by the actual wetted width at that cross section, and then multiplying by the average width of the segment's wetted area.

A simple count of the total units across each cross section does not create a metric with which to compare the lateral variability among the MUs, however. Therefore, for each section that contains a particular MU, the baseflow-width-normalized number of other MUs were summed and averaged for just those sections. If a unit tends to be large and dominate its locations, then the count of other MUs per cross section containing that unit may be low. On the other hand, if a unit tends to be small or slender, the coincident lateral count could be high.

5.6. Hydromorphic characteristics

In an effort to place the MUs in context with the channel geometry, their locations were compared with three hydromorphic characteristics: base-flow wetted width, water surface slope, and bankfull width–depth ratio. The water surface slope (WSS) is a key hydraulic feature that has been commonly used as an MU identifier in other studies, and is a proxy for riverbed slope. Width–depth (W/D) ratios are valuable for expressing channel hydraulic geometry relationships, as well as indicators of channel stability.

In order to relate the hydromorphic characteristics to an MU type, each cross section needed to be assigned to the MU that dominated it, if one existed. The total areas of each MU type within each cross-sectional rectangle were determined for the longitudinal analyses. An MU that consisted of at least 60% of the total area of each cross-sectional rectangle was considered to be the 'dominant' MU for that location. Thus, the mean hydromorphic characteristics for cross sections dominated by a particular MU type could be determined. Any cross section that did not exhibit a singular dominant MU was not used for these analyses.

The MU-averaged values were compared between all pairs of MUs using the nonparametric Mann-Whitney rank-sum U test. This statistical test involves ranking data and evaluating the sum of the ranks relative to random expectation in assessing the null hypothesis that two sets of samples come from identical populations (Freund and Simon, 1991; Pasternack and Brush, 1998). For this study, pairs of MU types were evaluated for statistical differences above the 99% confidence level ($p < 0.01$), above the 95% confidence level ($p < 0.05$), and below the 95% confidence level (i.e., statistically indifferent).

Mean wetted widths were calculated for each cross-sectional rectangle (section 5.2) and averaged for each type of MU among their respective dominated cross sections. Each width was then normalized by the segment-scale mean base-flow width.

Given variability of MU shapes and sizes, calculating the slope of every individual unit would not be meaningful, so the MU-dominated cross sections were used. Water surface elevation (WSE) is a 2D model output that can be converted into a raster. ArcGIS can then be used to calculate the mean WSE of each cross section. The WSS at each cross section is calculated as the difference in mean WSE between the two immediate upstream and downstream cross sections divided by the horizontal distance. For the case studies presented herein, all WSS values less than zero were removed, as these were considered to be local anomalies. MU-averaged WSS were thus calculated from the set of values generated among the representative cross sections for each MU type.

A width–depth ratio < 12 is considered low and > 40 is considered high (*sensu* Rosgen, 1996). The W/D was calculated based on wetted top width and mean depth during bankfull flow at each cross section. Cross sections that exhibited a dominant MU had their W/D ratios tabulated and analyzed, stratified by MU. Thus, the mean W/D ratio for cross sections dominated by a particular MU type could be determined, as well as the percent of all MU-dominated cross sections that exhibit a high or low value.

6. Results

6.1. Abundance and diversity

The MUs in the LYR exhibit an unequal abundance, in total number of polygons and total area (Table 2). Almost two-thirds of the total numbers of MU polygons were delineated as either slackwater or slow glide. These high values are likely because the slackwater and slow glide morphologies are such that they exist along the baseflow channel margins and therefore are typically long, slender regions that tend to be separated into multiple polygons during the delineation process owing to the square-pixilation effects. This is supported by the area histograms (Fig. 7) that show slackwater and slow glides comprise the greatest number of polygons of the smallest possible size (i.e., one pixel = 0.91 m x 0.91 m) as compared to the other MUs and the fact that these two units comprise only 28% of the total area (Table 2).

In terms of area, the three most abundant units were slackwater, pool, and riffle transition. Pool covered 15.9% of the segment area, despite having only 2.0% of the total number of delineated polygons, which indicates that pools are typically delineated as large cohesive units in the LYR. The three least abundant units in area were chute, run, and slow glide. Chute and run units also comprised low percentages of the total number of polygons. Slow glide, however, had the second highest number of polygons, which indicates that it is typically delineated as small discrete units.

Mean polygon sizes ranged from 19 to 404 m^2 for each unit type and maximum sizes ranged from 7220 to 71,746 m^2 by type (Table 2). Using the mean base-flow wetted width of 59.5 m, these areas can be normalized into representative length scale by taking the square root of the area then dividing by the mean flow width. The mean polygon sizes therefore range between 0.07 and 0.34 W. This calculation assumes a square unit, even though most of the mapped units in the LYR exhibit an irregular shape. The maximum size polygons range from 1.43 to 4.50 W. These sizes agree with the commonly accepted notion that morphological units are scaled on the order of ~ 1-10 W but also demonstrate that they can be smaller than previously understood on the basis of the spacing concept alone.

Area percentages of the MU types ranged from 4.3 to 16.4%; however, five of the eight are within a couple of percentage points of each other. The Shannon diversity (Eq. 1) for MUs on the LYR was 2.022 (as compared to a completely diverse value of 2.079). The evenness (Eq. 2) of polygon coverage was 0.973 (as compared to a fully even coverage value of 1.0), and the dominance (Eq. 3) value was 0.057 (as compared to a value of 0 for equal areas). The combination of these diversity indices shows no one particular MU type is dominating the segment area and that their population abundances are virtually equal, which is expected given the small range of abundance percentages. Whether MU equality constitutes MU randomness cannot be addressed with these metrics, so further testing was done.

This study utilizes a pixel size of 0.91 m x 0.91 m in ArcGIS to delineate MUs, which invariably resulted in some cases of a single pixel being characterized as an MU type and not adjacent other pixels of the same type (not considering diagonal pixels as adjacent). The area histograms (Fig. 7) show that this is true for all MU types. However, this small size could be considered more a discrete ‘hydraulic unit’ consisting of a highly localized landform at the next scale down of ~ 0.01-0.1 W. For most analyses, an MU landform should be readily identifiable in the field (e.g., Bisson et al., 1996). Because MUs are discretized using assessments of depth and velocity combinations derived from a 2D model at the 0.91 m x 0.91 m scale, an individual pixel whose depth and velocity combination forms a separate MU classification than all of its surrounding pixels could be considered either a real hydraulic unit or a model artifact caused by topographic noise (i.e., uncertainty at the meter scale) based on this delineation method rather than a fully realized MU landform. In fact, among all of the MU polygons, 45% are only one pixel in size (varying from 32% to 49% for each MU type). The cumulative area of these one-pixel polygons, however, account for only 0.76% of the channel. An easy argument can be made, then, that eliminating these one-pixel polygons from geomorphic analyses involving areas would have negligible effects on the results.

Further analysis was conducted to explore how large a delineated polygon must be in order to consider it a real landform on the LYR. With every increase in a minimum size threshold in terms of numbers of pixels or planform area, more total area of the channel would also be eliminated from geomorphic analysis. For example, setting the minimum size threshold at 23.4 m^2 (28 pixels, or ~ 4.8 m x 4.8 m), the total number of polygons excluded would be 90.1% and the total area excluded would be 5.1%. Increasing this threshold to 36.8 m^2 (44 pixels, or ~ 6.1 m x 6.1 m) yields an exclusion of 92.3% of the number of polygons and 6.4% of the area. The minimum polygon size threshold that would retain at least 90% of the channel's area was thought to be meaningful and a good whole number, and that turned out to be a size of 92.8 m^2 (111 pixels, or ~9.6 m x 9.6 m). This threshold would exclude 95% (another scientifically meaningful number) of the total number of polygons (Table 3); however, the high percentage of remaining area (90%) validates the concept that morphological units are on the commonly accepted scale of ~ 1-10 W in size and cover a majority of a channel's area. In addition to the minimum size of 92.8 m^2 retaining 90% of the channel area and excluding 95% of polygons for further analyses, this threshold size is also appropriately large enough for field surveyors to visually identify as a morphological landform (~ 1/6 W), and is consistent with sizes used in other delineation methods (e.g., Bisson et al., 1996; Thomson et al., 2001). After applying this minimum size threshold, the mean unit size for the remainder of each MU type ranged between ~ 0.4-0.8 W. Therefore, from a statistical and visual standpoint, the minimum size threshold for the following analyses for the LYR will be 92.8 m^2; however, as a comparison the same analyses described hence will also be performed using no size discrimination. In the following analyses, when the minimum size discrimination is applied, the subthreshold areas become unclassified and therefore not used.

6.2. Longitudinal distribution

Chutes and runs were more predominant above DPD (Fig. 8A, F) and less abundant toward the mouth. Slackwater (Fig. 8G) and slow glide (Fig. 8H) units were distributed close to uniformly across the full segment. Pools (Fig. 8C) were unequally distributed between the upper and lower regions but mostly lacking in the middle, except for the large forced scour hole immediately downstream of the DPD spillway. Riffles exhibited near-uniform probabilities through most of the segment, except for the upper- and lowermost regions (Fig. 8D). Riffle transitions (Fig. 8E) and fast glides (Fig. 8B) exhibited their highest occurrence near the DPD, but are otherwise fairly uniform. Overall, chutes and pools exhibited the most extreme deviations from a uniform distribution.

The same distribution functions were calculated using only the minimum, field-identifiable polygon size as determined in the previous subsection. Omitting the 10% of area associated with the smallest polygons, however, did not noticeably affect the longitudinal distribution percentages. The mean of the differences in percentages of areas at each cross section was 0.58%, with the greatest differences occurring for the slackwater (1.9%) and slow glide (1.2%) and the least for the run (0.02%) and chute (0.05%) distributions. These small differences did not affect the CDF slopes enough to alter the conclusions about the longitudinal distributions of each MU type along the channel. Therefore, the comparative distributions plots for the minimum size threshold are not presented here.

6.3. Longitudinal spacing

The longitudinal distribution results in section 6.2 show that some units, namely slackwater and slow glide, were so ubiquitous (i.e., near-uniform longitudinal distribution) and insufficiently longitudinally discrete for a test of spacing to be viable. Analysis of longitudinal spacing was therefore only performed for the six units that were distributed as longitudinally discrete units, i.e., chute, fast glide, pool, riffle, riffle transition, and run.

Histograms of the spacing lengths as expressed in terms of bankfull widths show unimodal distributions for each unit, with peaks between 2 and 3 W (Fig. 9). Mean spacings ranged from 2.7 to 4.4 W (runs and chutes are the respective end members). For direct comparisons with previous studies, the mean riffle and pool spacings were 3.3 and 4.3 W, respectively, which is less than the commonly accepted values of 5-7 W, but within range of the ~ 3 W reported by Carling and Orr (2000) for alluvial channels. For pool spacings, only ~ 29% of the sequences exhibited distances of 5-7 W, and the mode was between 2 and 5 W (~ 67% of all spacings). For riffles, ~ 18% of the spacings were between 5 and 7 W, with a mode of ~ 2-3 W (~ 46%). These results corroborate the hypothesis by Keller (1972) that longer sequences tend to be unstable and break up into smaller spacings in nonideal conditions. Also of note is that riffles and pools exhibited different mean and mode spacings, which indicates that they are not necessarily linked together as a coupled unit.

For units that were not riffle or pool, little literature exists with which to compare our values. Chutes had a distinct mode at 3 W and a mean of 4.4 W, but were spaced as far as 24 W. The fact that this has the largest mean may be because of its uneven distribution (Fig. 8), which shows that chutes are more abundant in the region just upstream of DPD. In fact, if DPD is used to separate the river segment into two reaches, then the mean chute spacings are 3.3 and 6.3 W for upstream and downstream of the dam, respectively. However, pools also exhibited a similarly uneven distribution, but the spacings upstream and downstream of DPD were not as different (4.2 and 4.5 W, respectively). Three units (pool, run, riffle transition) exhibited mean spacings that align with the mode (Fig. 9), which indicates that their locations are more stable and their recurrences more regular.

6.4. Adjacency

Adjacency results show that a strong organizational structure is evident (Table 4; Fig. 10). This could be an artifact of the classification metric; however, the metric was created with an eye to actual physical conditions, so this is likely a true representation of landform organization. A clear grouping of collocated steep, constricted units (i.e., riffle, run, and chute) emerged, whereas pools did not exhibit strong mutual collocations. Fast glide, riffle transition, and slow glide existed as buffers between the grouping of riffle–run–chute and the other unit types (Fig. 10A). Meanwhile, riffle→pool and pool→riffle adjacencies had greater-than-random avoidance (Table 4), which differs from traditional, simplistic methods for identifying only pool and riffle MUs in a channel.

The results in Table 4 include all MU polygons, regardless of size. To evaluate whether adopting the field-identifiable minimum size threshold affects these results, the same analysis was performed for just those MU polygons with areas > 92.8 m^2 (Table 5). The total number of adjacencies in the segment corridor is reduced to ~ 2.5% of the raw count. Most connections that were considered as scientifically significant collocations remained so (Fig. 10B). The two exceptions were riffle→slow glide and riffle transition→slackwater, which changed to avoidance and near-random, respectively. Two of the three previously near-random adjacencies changed to collocation (pool→slackwater and riffle→run), while the third changed to avoidance (riffle→slackwater). Six previous avoidance probabilities changed to greater-than-random collocation: riffle→chute; fast glide→run; riffle transition→fast glide; riffle transition→riffle; slackwater→pool; and slow glide→fast glide. Eight other adjacent combinations also increased from avoidance to near-random (Table 5).

6.5. Lateral variability

Considering that the mean MU sizes are < 1.0 W (section 6.1), we should expect laterally coherent MUs. Employing no minimum size discrimination of the MU polygons, the LYR exhibited an average of ~ 18 units per base-flow width (Fig. 11A). If the margin units are pixilated and separated from one cohesive unit into 5 or 6 diagonally adjacent units, then this number can be justified. In fact, on average ~ 57% of the polygons at each cross section were comprised of slackwater and slow glide units at this scale.

However, most field observers would likely have a difficult time visualizing that many units across an ~ 60-m channel (e.g., about one unit every 3 m). Applying the minimum field-identifiable MU size threshold, the average number of units per cross section decreases to a value of six (Fig. 11B). An example of how six MUs might occur across one cross section would be if there were slackwater and slow glide units along both banks bookending a mid-channel fast glide and pool (Fig. 4). The implication of this analysis is that any given cross section is not necessarily associated with any one MU, as is typically assumed and reported. Therefore each cross section does not exhibit any one combination of hydraulics and, therefore, not any one potential habitat. Instead, a complex and diverse suite of landforms and potential habitat exist at any given cross section in a gravel–cobble river. Capturing this spatial complexity is where 2D planview MU analysis has the most value. The statistical analyses herein reduce that complexity to scientifically meaningful metrics.

6.6. Hydromorphic characteristics

The lateral variability results show that each cross section was comprised of more than one MU. However, ~ 25% of the cross sections in the LYR were comprised of an MU that made up at least 60% of the area in the cross-sectional rectangle. Therefore, those cross sections were considered to contain a ‘dominant’ MU for the following analyses, and only those MU-dominated cross sections were analyzed for their relative hydromorphic characteristics.

The wetted width of representative cross sections also varied significantly by MU. Slackwater and riffle transition units tend to occur in wide channel sections (Table 6), while chutes and runs occur in narrower ones. MU-averaged widths were highly statistically different ($p < 0.01$) for 24 out of 28 MU pairs. The other four MU pairs that were statistically indifferent at the 95% confidence level involved slow glide (versus pool, riffle, and riffle transition), while the other one was between fast glide and riffle.

Cross sections dominated by riffles exhibit the highest WSS (Table 6), almost double that of the next highest (chute). Pools and slackwater cross sections exhibit the lowest mean slopes. Using a Mann-Whitney rank sum U test, mean slopes of 24 out of 28 pairs of MU types were highly statistically different ($p < 0.01$). Fast glide and slow glide were significantly different at the 95% confidence level ($p < 0.05$). The exceptions where mean slopes were statistically indistinct ($p > 0.05$) included riffle transition–run, fast glide–slackwater, and slow glide–slackwater.

The channel cross sections dominated by each MU type exhibited a very high bankfull width–depth ratio (i.e., > 40), except for pool (Table 6). Pool-dominated cross sections were also the only ones that exhibited any width–depth ratios < 12, and in fact, only 8.2% of the pool sections exhibited values > 40. Amongst the other MU types, a majority of their dominated cross sections exhibited width–depth ratios > 40 (ranging from ~ 75 to 100%). Only chute-dominated cross sections were all > 40 (Table 6).

Using a Mann-Whitney rank sum U test, mean width–depth ratios of 15 out of 28 pairs of MU types were highly statistically different ($p < 0.01$). Chute was significantly different ($p < 0.05$) from riffle transition and slow glide. Notably, pool was the only unit to exhibit high statistical significance from all the other MU types. The MU pairs that were statistically indifferent include: chute–riffle, chute–slackwater, fast glide–run, fast glide–

slackwater, fast glide–slow glide, riffle–slackwater, riffle transition–slackwater, riffle transition–slow glide, run–slackwater, run–slow glide, and slackwater–slow glide.

7. Discussion

Channel morphology is shaped by several complex and interrelated processes, such as upstream hydrology, transport capabilities of the substrate, channel–floodplain interactions, and flow hydraulics. While some inherent randomness might exist in these processes, the resulting morphological patterns are nonrandom and nonuniform, as exemplified by the analyses discussed herein. Each MU type exhibited some particular spatial organization characteristics within the LYR. The following subsections provide some context for interpreting these results.

7.1. Effect of imposing a minimum size for MUs

Previous field delineation procedures have typically set a minimum size for MUs subject to the user's ability to discern contiguous properties at a particular scale (e.g., Bisson et al., 1996). For the methodology used herein, the MUs are digitally delineated using a 0.91 m x 0.91 m pixel scale. However, it is suggested that an MU of this size is difficult to field-verify and does not constitute a reasonably discrete landform free of data collection noise. Therefore, a size of 92.8 m^2 was decided as a minimum scale for units in the LYR on the basis that it constituted the 90th percentile of polygon size. Spatial analyses were performed on the MUs using the raw and the thresholded sets of polygons, which thus introduces the question of whether this size discrimination affected the results and their associated interpretations.

Polygon segregation had the largest impact among analyses for slackwater and slow glide as they experienced the largest reductions in number of polygons and in total channel area (Table 3). The problem is that these are the long, skinny units that require a finer resolution than ~ 1 m to obtain multiple contiguous pixels forming coherent MU polygons of ~ 5 m width, given the overall width of the LYR. The order of MUs from largest to smallest in total area, excluding slackwater and slow glide, is the same irrespective of the minimum size application. However, an analysis including all polygons would show that slackwater is the most abundant, whereas pool covers the most area if only the field-identifiable sizes are used. Ignoring the areas that are comprised of a complex array of small units could have an impact on river management schemes, even if it is only 10% of the channel.

The interpretations of the longitudinal analyses for each unit do not change with minimum size segregation. This suggests that large polygons of any particular MU tend to be spatially associated with smaller polygons of the same type. Ignoring the smaller polygons, therefore, does not lead to ignoring whole areas where an MU is identifiably abundant.

For the adjacency analyses, the size segregation affects the large ↔ small polygon transitions. Removing the small polygons reduced the number of adjacencies by ~ 97.5%, which suggests that many large polygons were ringed by smaller, noncohesive units. The most significant impact is that the riffle → slow glide transition switched from statistically collocated to avoided. Conversely, a couple of adjacencies switched from avoidance to collocation using only the larger polygons, namely riffle → chute and slackwater → pool. Several other adjacencies switched from being statistically avoided to near-random (Tables 4 and 5). For the most part, the other adjacency distinctions remained the same.

The most extreme difference in results using the minimum size polygons is that for counting the number of MUs laterally across the channel. Using all polygons, the average number of MUs per cross section is almost 20, but that number reduces to about six if the smaller polygons are excluded. This difference, however, does not change the interpretation that large gravel–cobble rivers exhibit significant lateral variability in channel morphology, which has been neglected in the past but should now be accounted for in river science and management. Even with this size discrimination, every cross section exhibits more than one MU across its width. The ability to recognize this amount of lateral variability represents a shift in the manner in which river scientists have usually mapped channels.

In summary, using a minimum size threshold changes some of the details but not the overall results that MUs in a cobble-bed river exhibit a deterministic organizational pattern.

7.2. Base flow versus bankfull flow as a normalizing discharge

A decision was made for this study to use mean bankfull wetted width as the normalizing variable for longitudinal spacing analyses. An alternative would be to normalize by mean base-flow channel width, because that is the relevant discharge at which the MUs were identified and delineated. Other studies of unit spacings have also typically used the discharge at observation, which tends to be somewhere between base flow and bankfull and is usually called ‘active channel width’ (e.g., Grant et al., 1990). The question of which mean width to use depends on several factors. First, a single bankfull discharge may or may not be identifiable or appropriate for a given river, as a function of landscape context, disturbance regimes, and/or climate and climatic change. Second, as the lengths of study segments that can be accurately interpreted with 2D models increase, the hydrology within these study segments may be gaining or losing too much water to rely on a single discharge metric. This study spanned ~ 37 km of channel but was in a lowland context with no sizable unregulated tributaries. Third, the appropriate width to use may also hinge on whether the controlling hydraulics that influence MU organization occur during base flow, bankfull, or some other significantly larger discharge.

This decision, however, may influence the values calculated for the MUs in the LYR and, hence, comparisons to other systems. For comparison, therefore, the averaged longitudinal spacings for each MU were also normalized by mean base-flow width as a sensitivity test. The mean bankfull width for the LYR is 97.3 m, the mean base-flow width is 59.5 m (about 40% narrower), and the spacings are each altered by about this same amount (Table 7). Interestingly, the distances between successive units now become more comparable to previously published values of 5-7 W. Riffle spacings would be 5.4 W, and pools 7.0 W. The spacings for the other units also increase to within or near the 5-7 W range; however, without other studies with which to compare, what their expected values should be is difficult to know. Overall, insufficient data exist to set a standard at this time, so practitioners are recommended to use their judgment based on conditions in their study segment and be transparent in reporting their chosen discharge.

7.3. Syntheses of spatial patterns for each MU

By synthesizing the results by MU, a unique picture emerges for the observed pattern and organization of each unit within the LYR (Table 8). Above all else, this study found that the euphemism of a ‘riffle–pool unit’ certainly would be invalid for the LYR and likely for other rivers once analyzed in higher resolution using 2D MUs. Several of the spatial analyses presented herein highlight the lack of coupling between these units. First, pools occur in greater abundance than riffles in terms of planform area. Using the minimum size discrimination, pools are the most abundant unit while riffles are the fifth most (Table 3). Second, pools are spaced apart ~ 1-2 W more than riffles on average (Fig. 9). Third, pools and riffles are not spatially collocated to each other (Fig. 10). When viewed as laterally discrete landforms, riffles tend to group with chute and run. Because these three MU types have significantly different base-flow depths, the interpretation is that their common high velocities must be because of high slopes and/or local constrictions, which would be vertical for riffles and lateral for runs and chutes. Meanwhile, pools do not exist in a clear grouping, but show one-way adjacencies to fast and slow glides and a weaker bidirectional collocation with slackwater. The common term ‘riffle–pool unit’, therefore, should be reinterpreted reflecting its low resolution, reach-scale perspective to actually mean ‘a hole in part of the riverbed surrounded and followed by flatter areas and eventually transitioning to a steep, constricted region’. Because longitudinal profiles often arbitrarily follow the thalweg as opposed to the centerline or other streamline, they go through pools disproportionate to their actual areal presence (Table 2), giving pools more weight than they are possibly due.

Therefore, an important future direction should be explaining why large swaths of a channel are relatively flat compared to past work explaining why there exists holes and bumps in a thalweg profile, which are preferentially selected to capture those holes and bumps.

Looking beyond the narrow view of MU types dominated by riffles and pools, this study found interesting patterns for other unit types as well. Chutes, for example, occupied the smallest area of the LYR segment; tended to cluster upstream of DPD and avoided the mouth; exhibited the longest average spacing of about 4.4 W from each other; were preferentially adjacent to runs and riffles; and were laterally associated with less than five other MUs per cross section. The next most abundant units were runs that tended to cluster upstream of DPD and also avoided the mouth; exhibited the shortest average spacing of about 2.7 W from each other; were preferentially adjacent to fast glide, riffle, and riffle transition; and were laterally associated with over five other MUs per cross section. Slackwaters and slow glides were both near-uniformly distributed along the channel hugging the margin, with some slight clustering in the downstream regions; both exhibited adjacency collocations to each other and to riffle transitions; however slackwater tended to be laterally associated with fewer other MUs per cross section than slow glide. Fast glides and riffle transitions occupied about the same percentage of the segment area and had similar longitudinal spacing values, but differed in their preferential locations along the LYR: where fast glides tended to avoid the upstream bedrock regions and clustered around the DPD, and riffle transitions tended to avoid the mouth but were otherwise prevalent downstream of DPD.

7.4. Deterministic characteristics of MU patterns

The hydromorphic characteristics provide a synthesis of the channel morphology at locations in which a majority of the base-flow wetted width was dominated by a particular MU (Table 6). For example, pools tended to be located in deep areas with low water surface slopes. Riffles tended to occur in wide areas with high water surface slopes. Slackwater areas exhibited the highest base-flow wetted widths and high values of width–depth ratios. This signifies that slackwater units occurred in regions in which the valley base is very wide and flat, i.e., without a well-defined channel.

An important conclusion from this study is that MU patterns are nonrandom. The next logical question should then be, why? If a particular unit tends to cluster in or similarly avoid a certain region of the river, are there characteristics of the river valley that cause these patterns? Does this result then suggest that the patterns are therefore deterministic, i.e., qualitatively predictable? The mechanistic origins of these units are still poorly understood, but it was previously demonstrated that flow convergence routing was existent in at least one pool–riffle–run sequence on the LYR (Sawyer et al., 2010); and consistent with that mechanism, the longitudinal positioning of riffle crests in Timbuctoo Bend (Fig. 1) has persisted for decades (White et al., 2010). A full understanding of such mechanisms is beyond the scope of this study, but a strong case can be made that any such mechanism that is dependent on multiscale landscape heterogeneity will require a spatially explicit and sufficiently objective method for characterizing landforms, such as the approach demonstrated in this study.

7.5. Future directions

Once an accurate map of the landforms has been established, it can be used to stratify biologic and stage-dependent hydraulic data sets and as a baseline for future geomorphic change analyses. The LYR MU map has previously been incorporated into studies of the riparian vegetation (Abu-Aly et al., 2013) and spawning habitat suitability for Chinook salmon (Pasternack et al., 2013). Any comprehensive landform map can serve as the basis for a 'bottom-up' approach to understanding and linking the channel morphology with the ecologic habitat and can guide river management and rehabilitation strategies.

For this study, the MUs were mapped and analyzed only within the base-flow region of the LYR. However, rivers are more than just their base-flow channels; and if the spatial scope were to increase outward to the valley walls, other landform types would become included, such as bars, swales, and floodplains, etc. The purpose of this study was to highlight the inherent spatial organization of in-channel landforms, and the same analyses reported here could translate to a broader study that includes bankfull and out-of-channel MUs. Wyrick and Pasternack (2012) extended the in-channel methods and concept presented herein to the entire river corridor, but the full scope of that analysis is beyond what could be presented at this time.

8. Conclusions

The MUs represent distinct form–process associations and are important links in hierarchical morphology frameworks. Gravel–cobble rivers exhibit a high diversity of landforms; however, each MU type differs in streamwise distribution and spacing, adjacency collocations and avoidances, and lateral variability. Each MU type tends to preferentially occur within regions of distinct valley and channel characteristics.

Because of the near-census approach to surveying and modeling our study site, the results of the digital delineation and subsequent spatial analyses are scaled to sizes much smaller than what field methods produce, therefore creating maps that are more detailed and ultimately more accurate than large-scale averaging. Thus, this study highlights several key advances to the science and analysis of river morphology organization, some of which may seem to confute traditional knowledge but are a result of this increased resolution. First, a diverse suite of MU types that can comprise a river channel exist, not just pools and riffles. This point is particularly important for recognizing the inherent complexity of a channel's morphology and the relative role that plays in management strategies. Second, because the traditional pool–riffle morphology has persisted throughout the literature, spatial organization analyses of other MU types are lacking. Therefore, this study starts the discussion on the geospatial context for other MUs, such as runs, glides, and chutes. Third, all of the MU types exhibit a nonrandom spatial organization, indicating a natural structure to the channel morphology of a gravel–cobble river. Fourth, a cross section is often not defined by a single MU type. The discovery of laterally explicit MU variation represents an important link to the ecologic function of rivers. Fifth, the MU map is robust enough that the interpretation of the spatial organization does not significantly change by imposing a minimum size threshold on the delineated polygons to be used in the analyses.

Acknowledgements

Funding for this study was provided by the Yuba County Water Agency. Extensive knowledge and experience of the LYR that helped finalize the MU thresholds, and maps were provided by a consortium of experts that make up the Yuba River Accord Management Team (more information available at www.yubaaccordrmt.com).

References

Abu-Aly, T.R., Pasternack, G.B., Wyrick, J.R., Barker, R., Massa, D., Johnson, T., 2013. Effects of LiDAR-derided, spatially-distributed vegetative roughness on 2D hydraulics in a gravel-cobble river at flows of 0.2 to 20 times bankfull. Geomorphology, http://dx.doi.org/10.1016/j.geomorph.2013.10.017.

Barker, J.R., 2011. Rapid, abundant velocity observation to validate million-element 2D hydrodynamic models. M.S. Thesis, University of California at Davis, Davis, CA.

Bisson, P.A., Montgomery, D.R., Buffington, J.M., 1996. Valley segments, stream reaches, and channel units. In: Hauer, F.R., Lanberti, G.A. (Eds.), Methods in Stream Ecology. Academic Press, San Diego, CA, USA, pp. 23-52.

Borsanyi, P., Alfredson, K., Harby, A., Ugedal, O., Kraxner, C., 2004. A meso-scale habitat classification method for production modeling of Atlantic salmon in Norway. Hydroécologie Appliqué 14 (1), 119-138.

Carley, J.K., Pasternack, G.B., Wyrick, J.R., Barker, J.R., Bratovich, P.M., Massa, D.A., Reedy, G.D., Johnson, T.R., 2012. Significant decadal channel change 58–67 years post-dam accounting for uncertainty in topographic change detection between contour maps and point cloud models. Geomorphology, doi:10.1016/j.geomorph.2012.08.001.

Carling, P.A., Orr, H.G., 2000. Morphology of riffle-pool sequences in the river Severn, England. Earth Surface Processes and Landforms 25, 369-384.

Frissell, C.A., Liss, W.J., Warren, C.E., Hurley, M.D., 1986. A hierarchical framework for stream habitat classification: viewing streams in a watershed context. Environmental Management 10 (2), 199-214.

Grant, G.E., Swanson, F.J., Wolman, M.G., 1990. Pattern and origin of stepped-bed morphology in high-gradient streams, western Cascades, Oregon. Geological Society of America Bulletin 102, 340-352.

Gray, M., 2004. Geodiversity: Valuing and Conserving Abiotic Habitats. Wiley, Chichester, UK.

Gregory, K.J., Gurnell, A.M., Hill, C.T., Tooth, S., 1994. Stability of the pool-riffle sequence in changing river channels. Regulated Rivers: Resources Management 9, 35-43.

Halwas, K.L., Church, M., 2002. Channel units in small, high gradient streams on Vancouver Island, British Columbia. Geomorphology 43, 243-256.

Hauer, C., Mandlburger, G., Habersack, H., 2009. Hydraulically related hydro-morphological units: description based on a new conceptual mesohabitat evaluation model (MEM) using LiDAR data as geometric input. River Research and Applications 25, 29-47.

Hawkins, C.P., Kershner, J.L., Bisson, P.A., Bryant, M.D., Decker, L.M., Gregory, S.V., McCullough, D.A., Overton, C.K., Reeves, G.H., Steedman, R.J., Young, M.K., 1993. A hierarchical approach to classifying habitats in small streams. Fisheries 18(6), 3-12.

James, L.A., Singer, M.B., Ghoshal, S., Megison, M., 2009. Historical channel changes in the lower Yuba and Feather Rivers, California: long-term effects of contrasting river-management strategies, In: James, L.A., Rathburn, S.L., Whittecar, G.R. (Eds.), Management and Restoration of Fluvial Systems with Broad Historical Changes and Human Impacts. Geological Society of America Special Paper 451, pp. 57-81, doi: 10.1130/2008.2451(04).

Keller, E.A., 1972. Development of alluvial stream channels: a five-stage model. Geological Society of America Bulletin 83 (5), 1531-1536.

Keller, E.A., Melhorn, W.N., 1978. Rhythmic spacing and origin of pools and riffles. Geological Society of America Bulletin 89 (5), 723-730.

Klaar, M.J., Maddock, I., Milner, A.M., 2009. The development of hydraulic and geomorphic complexity in recently formed streams in Glacier Bay National Park, Alaska. River Research and Applications 25, 1331-1338.

Knighton, D., 1998. Fluvial Forms and Processes: A New Perspective. Edward Arnold Publishers Ltd, London, UK.

Lai, Y.G., 2008. SRH-2D version 2: Theory and User's Manual. U.S. Department of the Interior, Bureau of Reclamation, Technical Service Center, Denver, CO.

Leopold, L.B., Wolman, G.M., Miller, J.P., 1964. Fluvial Processes in Geomorphology. W.F. Freeman and Company, San Francisco, CA, USA.

Maddock, I., 1999. The importance of physical habitat assessment for evaluating river health. Freshwater Biology 41, 373-391.

Maddock, I., Smolar-Zvanut, N., Hill, G., 2008. The effect of flow regulation on the distribution and dynamics of channel geomorphic units (CGUs) and implications for

Marble Trout (*Salmo marmoratus*) spawning habitat in the Soĉa River, Slovenia. IOP Conference Series: Earth and Environmental Science 4, 1-10.

Madej, M.A., 2001. Development of channel organization and roughness following sediment pulses in single-thread, gravel bed rivers. Water Resources Research 37 (8), 2259-2272.

Milan, D.J., Heritage, G.L., Large, A.R.G., Entwistle, N.S., 2010. Mapping hydraulic biotopes using terrestrial laser scan data of water surface properties. Earth Surface Processes and Landforms 35, 918-931.

Moir, H.J., Pasternack, G.B., 2008. Relationships between mesoscale morphological units, stream hydraulics and Chinook salmon (*Oncorhynchus tshawytscha*) spawning habitat on the lower Yuba River, California. Geomorphology 100, 527-548.

Moir, H.J., Pasternack, G.B., 2010. Substrate requirements for spawning Chinook salmon (*Oncoryhnchus Tshawytscha*) are dependent on local channel hydraulics. River Research and Applications 26, 456-468.

Montgomery, D.R., Buffington, J.M., Smith, R.D., Schmidt, K.M., Pess, G., 1995. Pool spacing in forest channels. Water Resources Research 31 (4), 1097-1105.

Newson, M.D., Large, A.R.G., 2006. 'Natural' rivers, 'hydromorphological quality' and river restoration: a challenging new agenda for applied fluvial geomorphology. Earth Surface Processes and Landforms 31, 1606-1624.

Newson, M.D., Newson, C.L., 2000. Geomorphology, ecology and river channel habitat: mesoscale approaches to basin-scale challenges. Progress in Physical Geography 24 (2), 195-217.

O'Neill, M.P., Abrahams, A.D., 1984. Objective identification of pools and riffles. Water Resources Research 20 (7), 921-926.

Parker, G., 1976. On the cause and characteristic scales of meandering and braiding in rivers. Journal of Fluid Mechanics 76 (3), 457-480.

Pasternack, G.B., 2008. SHIRA-Based River Analysis and Field-Based Manipulative Sediment Transport Experiments to Balance Habitat and Geomorphic Goals on the Lower Yuba River. Cooperative Ecosystems Studies Unit (CESU) 81332 6 J002 Final Report, University of California at Davis, Davis, CA, 569 pp.

Pasternack, G.B., 2009. Specific Sampling Protocols and Procedures for Topographic Mapping. The Lower Yuba River Accord Planning Team, Marysville, CA.

Pasternack, G.B., 2011. 2D Modeling and Ecohydraulic Analysis. Createspace, Seattle, WA.

Pasternack, G.B., Tu, D., Wyrick, J.R., 2013. Chinook adult salmon spawning physical habitat of the lower Yuba River. Prepared for The Lower Yuba River Accord River Management Team, University of California, Davis, CA. Available at www.yubaaccordrmt.com.

Reid, H.E., Gregory, C.E., Brierley, G.J., 2008. Measures of physical heterogeneity in appraisal of geomorphic river condition for urban streams: Twin Streams catchment, Auckland, New Zealand. Physical Geography 29 (3), 247-274.

Richards, K.S., 1976. The morphology of riffle-pool sequences. Earth Surface Processes and Landforms 1, 71-88.

Rosgen, D., 1996. Applied River Morphology. Wildland Hydrology, Pagosa Springs, CO, USA.

Sawyer, A.M., Pasternack, G.B., Moir, H.J., Fulton, A.A., 2010. Riffle-pool maintenance and flow convergence routing observed on a large gravel-bed river. Geomorphology 114, 143-160.

Schwartz, J.S., Herricks, E.E., 2008. Fish use of ecohydraulic-based mesohabitat units in a low gradient Illinois stream: implications for stream restoration. Aquatic Conservation: Marine and Freshwater Ecosystems 18, 852-866.

Thompson, A., 1986. Secondary flows and the pool-riffle unit: a case study of the processes of meander development. Earth Surface Processes and Landforms 11 (6), 631-641.

Thomson, J.R., Taylor, M.P., Fryirs, K.A., Brierley, G.J., 2001. A geomorphological framework for river characterization and habitat assessment. Aquatic Conservation-Marine and Freshwater Ecosystems 11 (5), 373-389.

Wadeson, R.A., 1994. A geomorphological approach to the identification and classification of instream flow environments. Southern African Journal of Aquatic Sciences 20, 38-61.

Wadeson, R.A., Rowntree, K.M., 1998. Application of the hydraulic biotope concept to the classification of instream habitats. Aquatic Ecosystems Health and Management 1, 143-157.

White, J.Q., Pasternack, G.B., Moir, H.J., 2010. Valley width variation influences riffle-pool location and persistence on a rapidly incising gravel-bed river. Geomorphology 121, 206-221.

Wyrick, J.R., Pasternack, G.B., 2012. Landforms of the Lower Yuba River. Prepared for the Yuba Accord River Management Team, University of California, Davis. Available at www.yubaaccordrmt.com.

Zimmer, M.P., Power, M., 2006. Brown trout spawning habitat preferences and redd characteristics in the Credit River, Ontario. Journal of Fish Biology 68, 1333-1346.

Figure Titles

Fig. 1. Location map of the Lower Yuba River (LYR).

Fig. 2. Flowchart of MU delineation procedure. Parallelograms represent prepared data input; trapezoids represent manual input; diamonds represent decisions.

Fig. 3. Hydraulic thresholds for delineating MUs within the LYR at the selected base flow discharge.

Fig. 4. A sample location of the LYR's MU map that includes the cross-sectional boxes used for the longitudinal distribution and lateral variability analyses.

Fig. 5. A sample MU sequence that illustrates an example of an MU type (riffle transition) being located as two separate polygons on opposite sides of the channel from each other. For the longitudinal spacing analyses, this duad was combined into one unit. The black line represents the base-flow thalweg.

Fig. 6. A theoretical schematic of lateral MU variability within a channel. For the adjacency analyses, unit A would exhibit three transitions to unit B; however, the three units B all touch the same unit A and would therefore only count as one transition.

Fig. 7. Histograms of the individual polygon areas delineated for each MU type. The dashed line represents the cumulative percent area.

Fig. 8. Longitudinal distributions for each MU type based on percent of total area within each cross-sectional box (e.g., Fig. 4). The gray lines represent the discrete percentages of areas for each cross section. The dark black line represents the cumulative percentages of areas as measured from the mouth to the top of the segment. The diagonal lines represent a theoretical uniform cumulative distribution.

Fig. 9. Histograms of the sequential streamwise distances between like units. The absolute distances were normalized by the mean channel bankfull width. Any spacings in the ‘15’ column actually represent spacings of ‘15 or more’ channel widths.

Fig. 10. Collocation adjacency diagrams between MUs using (A) all delineated polygons, and (B) only the polygons larger than the minimum size threshold. For a full summary of adjacencies, refer to Tables 3 and 4.

Fig. 11. Total number of MU polygons within each cross-sectional box (e.g., Fig. 4) using (A) all delineated polygons, and (B) only the polygons larger than the minimum size threshold. The dark lines represent the segment averages.

Table 1
Descriptions of morphological units that occur within the LYR

Morphological unit	Description at base flow
pool	Topographic low in the channel that exhibits high depth and low velocity, and low water surface slope. This unit covers ‘forced pool’ and ‘pool’. A forced pool is one that is typically along the periphery of the channel and is ‘over-deepened’ from local convective acceleration and scour during floods that is often associated with static structures such as wood, boulders, and bedrock outcrops. A pool is not formed by a forcing obstruction. The distinction between forced pool and pool cannot be made automatically within GIS.
riffle	An area with shallow depths, moderate to high velocities, rough water surface texture, and steep water surface slope. Riffles are generally associated with the crest and backslope of a transverse bar (e.g., Knighton, 1998).
run	An area with moderate velocity, high depths, and moderate water surface slope. Runs typically occur in straight sections that exhibit a moderate water surface texture and tend not to be located over transverse bars.
chute	An area of high velocity, steep water surface slope, and moderate to high depth located in the channel thalweg. Chutes are often located at an abrupt vertical expansion.
fast glide	An area of moderate velocity and depth and low water surface slope. Fast glides commonly occur along the periphery of channels and flanking pools. Fast glides can also exist in straight sections of low bed slope.
slow glide	An area of low velocity, low to moderate depths, and low water surface slope. Slow glides may be located near water’s edge as other MUs along the channel thalweg transitions laterally towards the stream margins.
slackwater	A shallow, low velocity region of the stream that is typically located within adjacent embayments, side channels, or along channel margins. Velocities are near stagnant during base flow conditions and rise more slowly than in other units as stage increases.
riffle transition	Typically a transitional area between an upstream MU into a riffle or from a riffle into a downstream MU. Water depth is relatively low. Velocity is also relatively low, but increases downstream due to convective acceleration toward a shallow riffle crest that is caused by lateral and vertical flow convergence. The upstream limit is at the approximate location where there is a transition from a divergent to convergent flow pattern. The downstream limit is at the slope break of the channel bed termed the ‘riffle crest’.

Table 2

Area and size statistics of morphological units

Morphological unit	Total area (ha)	Number (-)	Maximum (m^2)	Median (m^2)	Mean (m^2)	Polygon size threshold for 90% of total MU area (m^2)
chute	8.86	606	7,220	4.2	146	185
fast glide	29.4	2,919	19,394	1.7	101	195
pool	32.9	814	71,746	2.5	404	936
riffle	27.2	1,988	8,998	2.5	137	268
riffle transition	31.7	6,604	28,060	1.7	48.1	78.6
run	17.9	1,455	7,784	1.7	123	204
slackwater	33.8	13,686	18,600	1.7	24.8	24.2
slow glide	24.7	12,981	12,598	1.7	19.1	14.2
All units	206.5	41,053	71,746	1.7	50.5	92.8

Table 3

Area and number of polygons delineated as each corresponding MU type for abundance analyses that include all mapped polygons (left side) and only those polygons larger than a field-identifiable size of 92.8 m^2 (right side)

	All MU polygons				Only MUs larger than minimum threshold			
Morphological unit	Area (ha)	Area (%)	Number (-)	Number (%)	Area (ha)	Area (%)	Number (-)	Number (%)
chute	8.86	4.3	606	1.5	8.33	4.5	116	6.0
fast glide	29.4	14.2	2,919	7.1	27.3	14.7	214	11.0
pool	32.9	15.9	814	2.0	32.3	17.4	134	6.9
riffle	27.2	13.2	1,988	4.8	25.9	13.9	228	11.7
riffle transition	31.7	15.4	6,604	16.1	28.2	15.2	301	15.5
run	17.9	8.7	1,455	3.5	16.8	9.1	194	10.0
slackwater	33.8	16.4	13,686	33.3	27.7	14.9	445	22.9
slow glide	24.7	12.0	12,981	31.6	19.3	10.4	311	16.0
Total LYR	206.5		41,053		185.9		1,943	

Table 4
Adjacency probabilities between the starting unit (left column) to all other units (top row). Grayed boxes represent values that are much larger than random (~ > 1.6), i.e., a ‘collocation’. Values much less than random (~ < 0.4) represent an ‘avoidance’. Results shown here include all MU polygons, regardless of size.

	chute	fast glide	pool	riffle	riffle trans	run	slack water	slow glide
chute	--	0.5	0.1	2.8	0.6	3.9	0.0	0.2
fast glide	0.1	--	0.7	0.5	3.2	0.7	0.7	2.3
pool	0.1	2.8	--	0.0	0.3	0.6	1.2	3.1
riffle	0.4	0.4	0.0	--	3.1	1.0	1.1	2.0
riffle trans	0.0	0.7	0.0	0.5	--	0.2	3.0	3.6
run	0.5	2.5	0.6	2.3	1.6	--	0.1	0.3
slackwater	0.0	0.2	0.1	0.2	1.9	0.0	--	5.6
slow glide	0.0	0.6	0.1	0.2	2.1	0.1	4.9	--

Table 5
Adjacency probabilities between the starting unit (left column) to all other units (top row). Grayed boxes represent values that are much larger than random (~ > 1.6), i.e., a 'collocation'. Values much less than random (~ < 0.4) represent an 'avoidance'. Results shown here include only the MU polygons larger than the minimum size threshold.

	chute	fast glide	pool	riffle	riffle trans	run	slack water	slow glide
chute	--	0.0	0.2	4.1	0.0	3.7	0.0	0.0
fast glide	0.0	--	1.1	0.8	2.5	1.4	0.1	2.1
pool	0.1	2.1	--	0.0	0.0	1.0	2.5	2.3
riffle	1.6	1.0	0.0	--	2.9	2.4	0.0	0.1
riffle trans	0.0	1.6	0.0	1.9	--	1.2	1.1	2.1
run	1.1	1.8	0.9	2.2	2.0	--	0.0	0.0
slackwater	0.0	0.2	1.5	0.1	1.7	0.0	--	4.6
slow glide	0.0	1.6	0.9	0.0	2.2	0.0	3.3	--

Table 6

Summary of physical channel characteristics at cross sections associated with each MU type. Bold values represent the maximum within each column and underlined values represent the minimum.

Morphological unit	Water surface slope (%)	Ratio of base flow wetted width to mean width	Bankfull width–depth ratio		
			Mean	% < 12	% > 40
chute	0.416	0.47	113	0	**100**
fast glide	0.038	0.96	73	0	75.3
pool	0.013	0.93	26	**1.2**	8.2
riffle	**0.765**	0.94	**114**	0	93.4
riffle transition	0.124	1.14	89	0	93.6
run	0.118	0.78	82	0	83.1
slackwater	0.027	**1.58**	90	0	91.7
slow glide	0.030	1.00	64	0	85.7

Table 7
Comparison of the means and modes for longitudinal spacings between like MUs as normalized by either the mean channel bankfull width or mean channel baseflow width

Morphological unit	Normalized by bankfull width		Normalized by base-flow width	
	Mean	Mode	Mean	Mode
chute	4.4	3	7.1	4
fast glide	3.0	2-3	4.9	2-5
pool	4.3	2-5	7.0	3-8
riffle	3.3	2-3	5.4	4
riffle transition	3.2	2-4	5.2	3-4
run	2.7	2	4.3	2-3

Table 8

Summary of the spatial organizations for each MU, using the minimum size threshold for the polygons. The data in column 2 are synthesized from Table 2; column 3 from Fig. 8; column 4 from Fig. 9; column 5 from Table 4; and column 6 is the average number of other MUs within a cross section that also contains the starting MU.

Morphological unit	Abundance (% segment area)	Longitudinal distribution	Longitudinal spacing (W)	Adjacency (**collocation to**, *avoidance of*)	Lateral variability (avg # of other MU per cross-section)
chute	4.5	avoidance near mouth; preference u/s of DPD	4.4	**run, riffle** *all others*	4.7
fast glide	14.7	avoidance in u/s bedrock region; preference near DPD	3.0	**riffle transition, run, slow glide** *chute, slackwater*	5.0
pool	17.4	avoidance in middle near DPD; preference near mouth and upper bedrock reaches	4.3	**fast glide, slackwater, slow glide** *chute, riffle, riffle trans.*	3.8
riffle	13.9	avoidance near mouth and Englebright Dam; preference u/s of DPD	3.3	**riffle trans., run, chute** *pool, slackwater, slow glide*	4.7
riffle transition	15.2	avoidance near mouth; preference d/s of DPD	3.2	**fast glide, riffle, slow glide, slackwater** *chute, pool*	4.6
run	9.1	avoidance near mouth; preference u/s of DPD	2.7	**fast glide, riffle, riffle transition** *slackwater, slow glide*	5.3
slackwater	14.9	no avoidance; some preference d/s of DPD	*n/a*	**riffle transition, slow glide, pool** *all others*	4.1
slow glide	10.4	no avoidance; some preference d/s of DPD	*n/a*	**fast glide, riffle transition, slackwater** *chute, riffle, run*	4.8

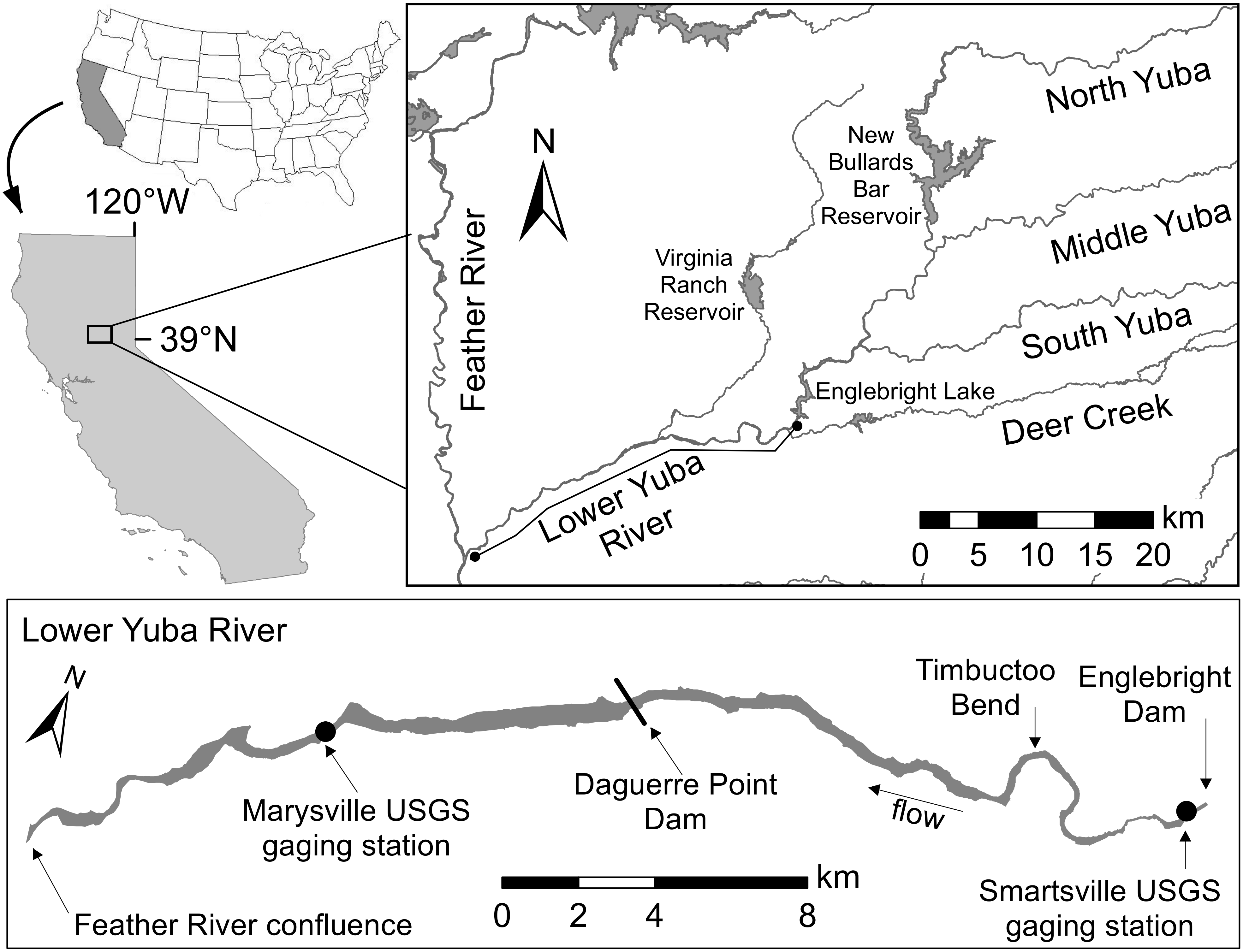

120°W
39°N
N
Feather River
North Yuba
New
Bullards
Bar
Reservoir
Middle Yuba
Virginia
Ranch
Reservoir
South Yuba
Englebright Lake
Deer Creek
Lower Yuba
River
km
0
5
10
15
20
Lower Yuba River
N
Timbuctoo
Bend
Englebright
Dam
Marysville USGS
gaging station
Daguerre Point
Dam
flow
Smartsville USGS
gaging station
Feather River confluence
km
0
2
4
8

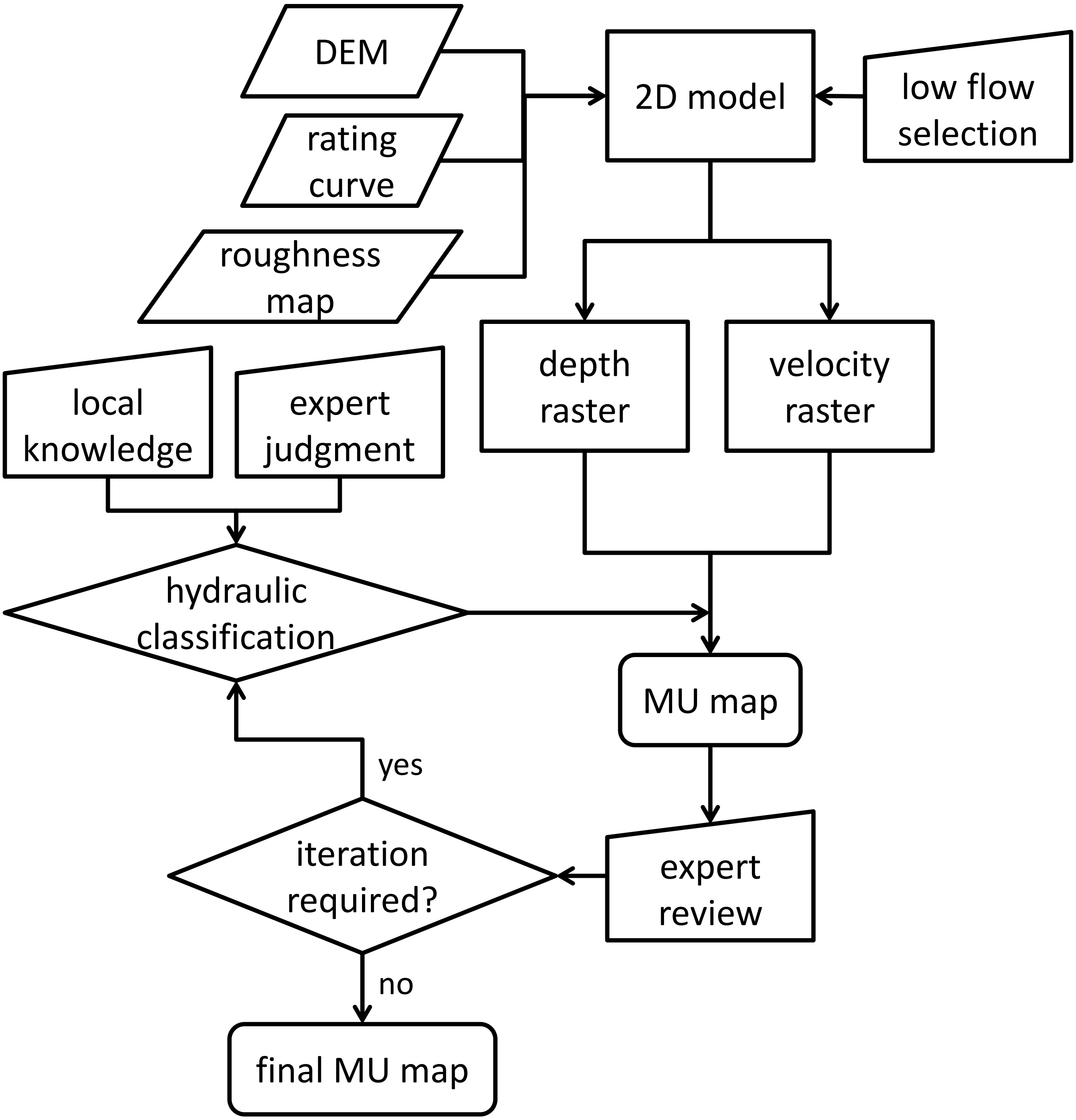
DEM
rating curve
roughness map
2D model
low flow selection
depth raster
velocity raster
local knowledge
expert judgment
hydraulic classification
MU map
expert review
iteration required?
yes
no
final MU map

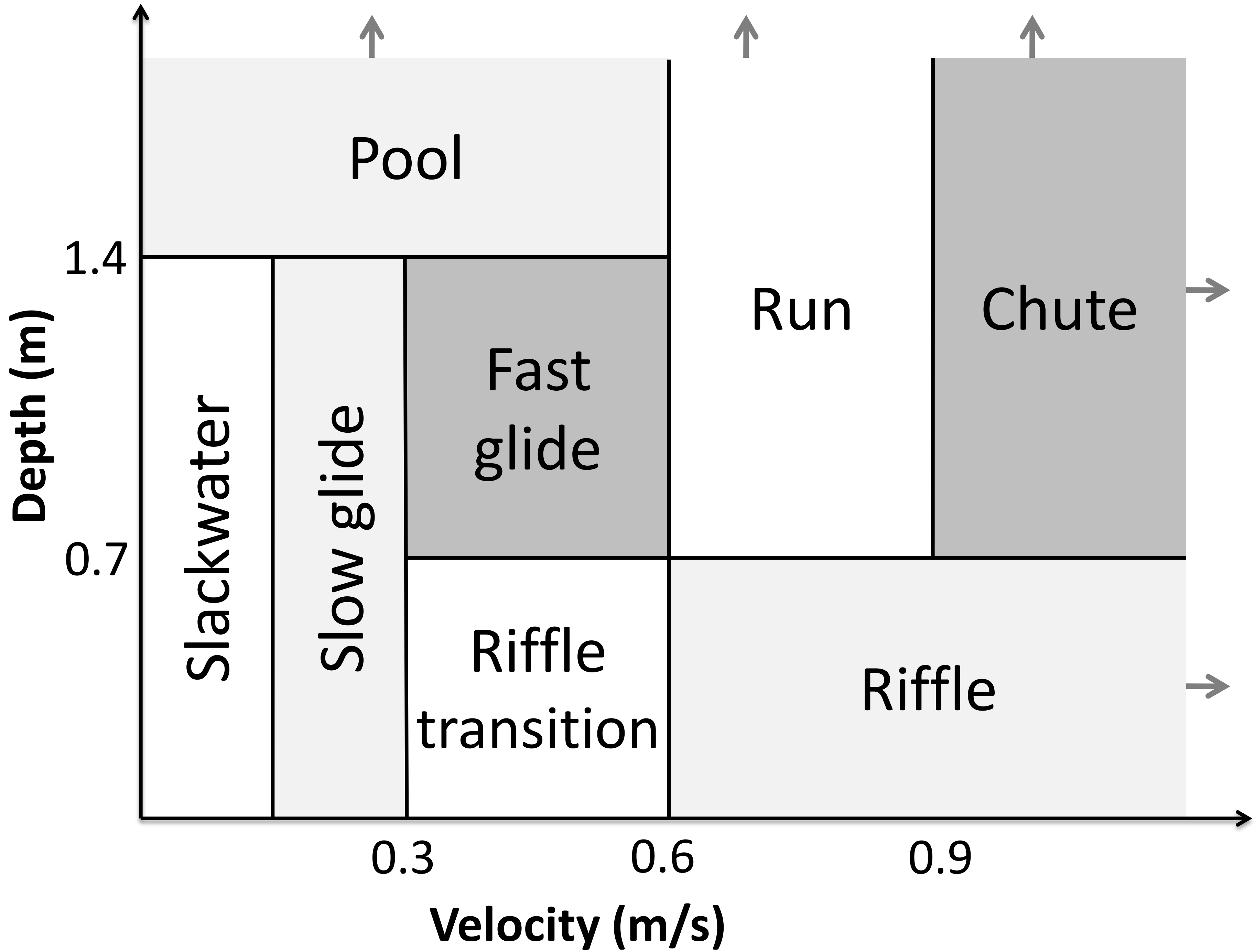
Pool
Slackwater
Slow glide
Fast glide
Riffle transition
Run
Chute
Riffle
1.4
0.7
Depth (m)
0.3
0.6
0.9
Velocity (m/s)

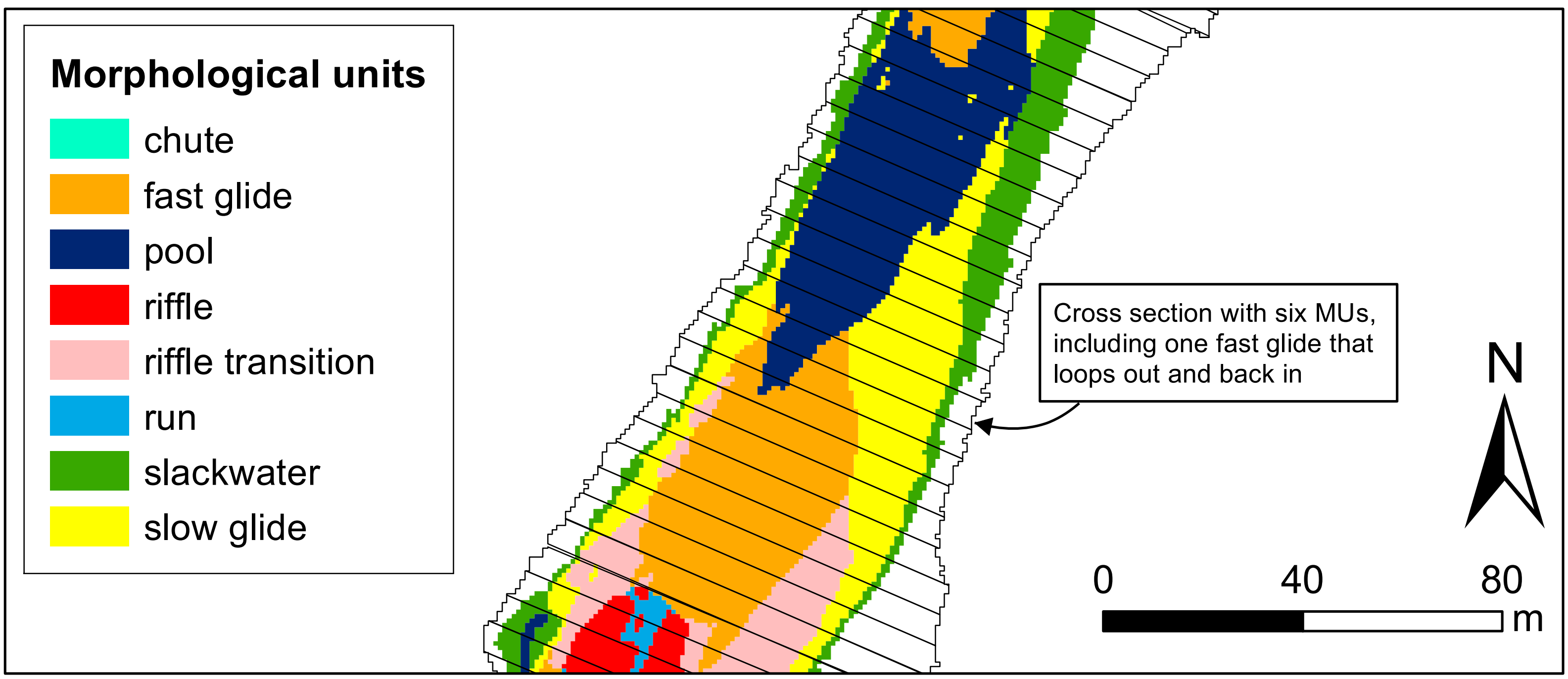

Morphological units
chute
fast glide
pool
riffle
riffle transition
run
slackwater
slow glide
Cross section with six MUs, including one fast glide that loops out and back in
N
0
40
80
m

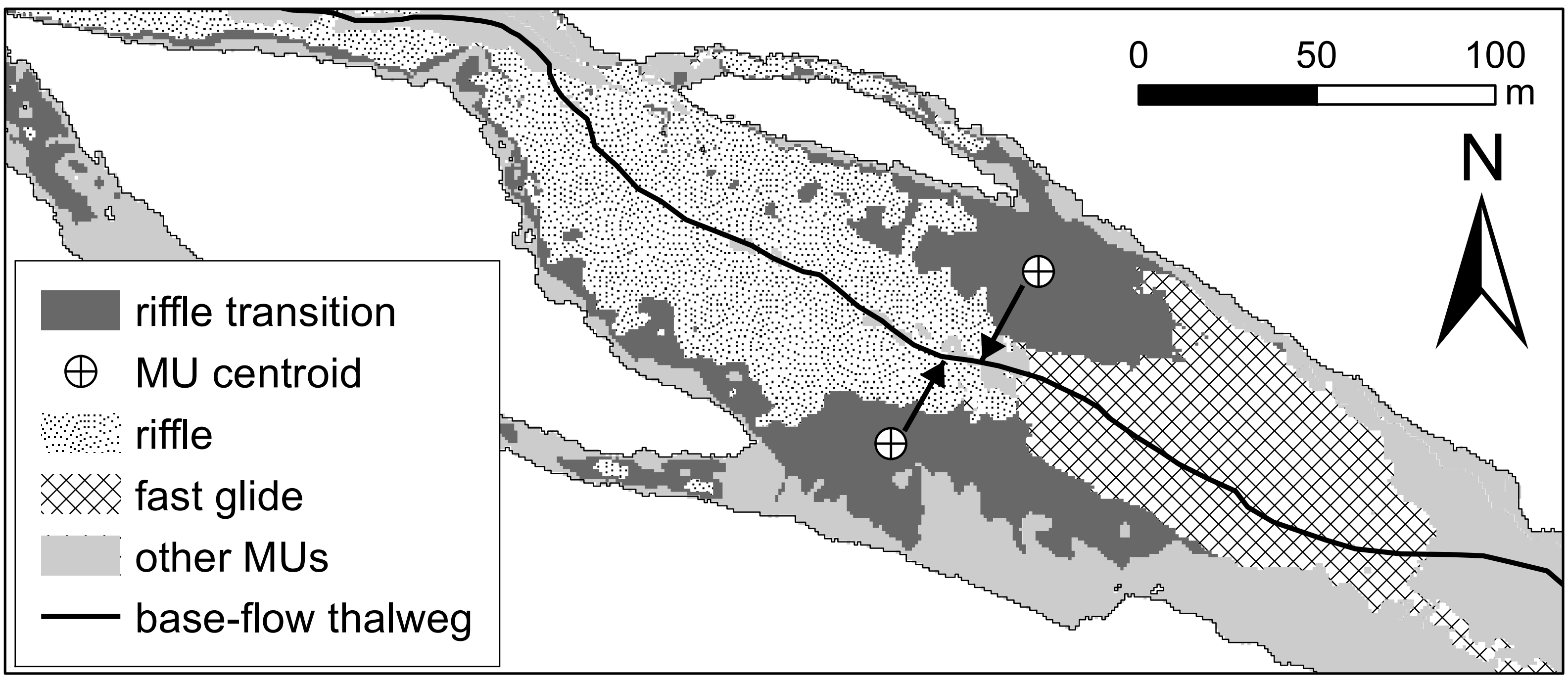

0
50
100
m
N
riffle transition
MU centroid
riffle
fast glide
other MUs
base-flow thalweg

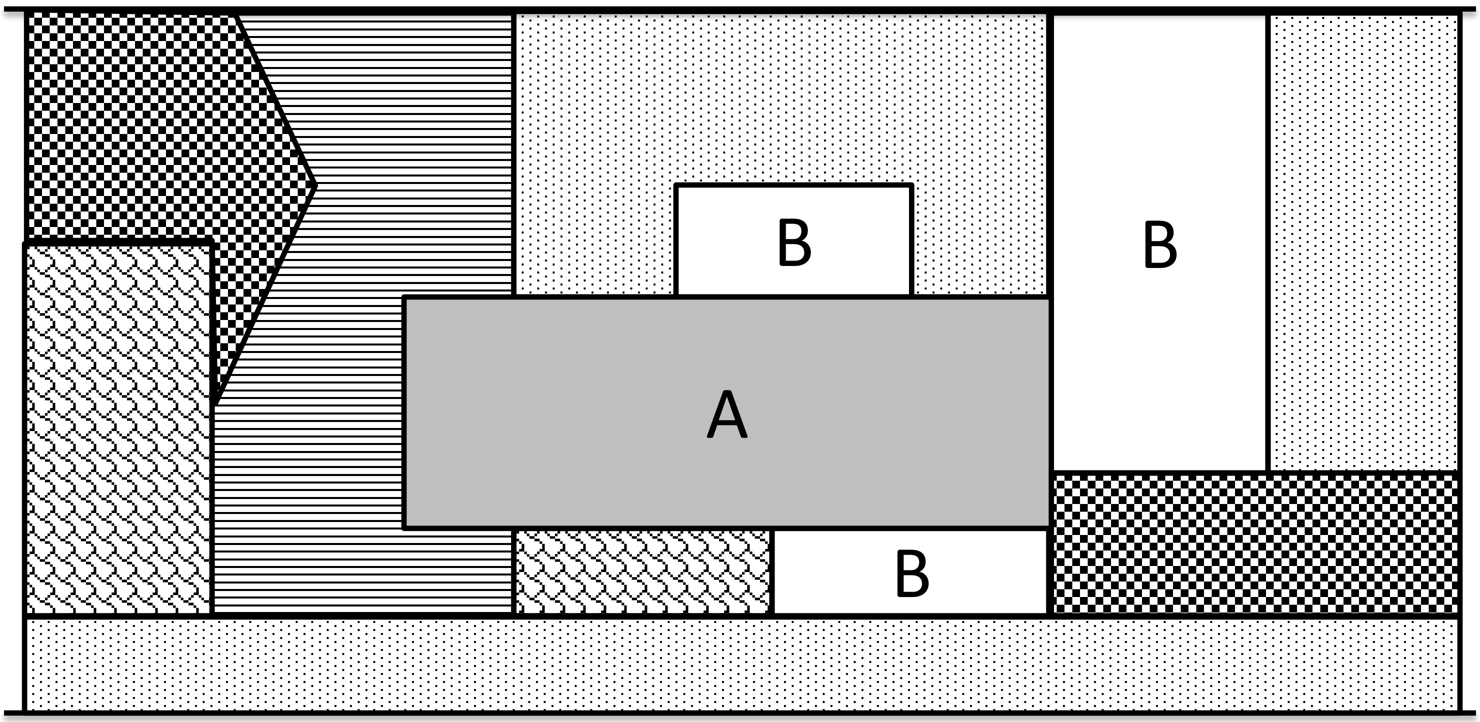
B
B
A
B

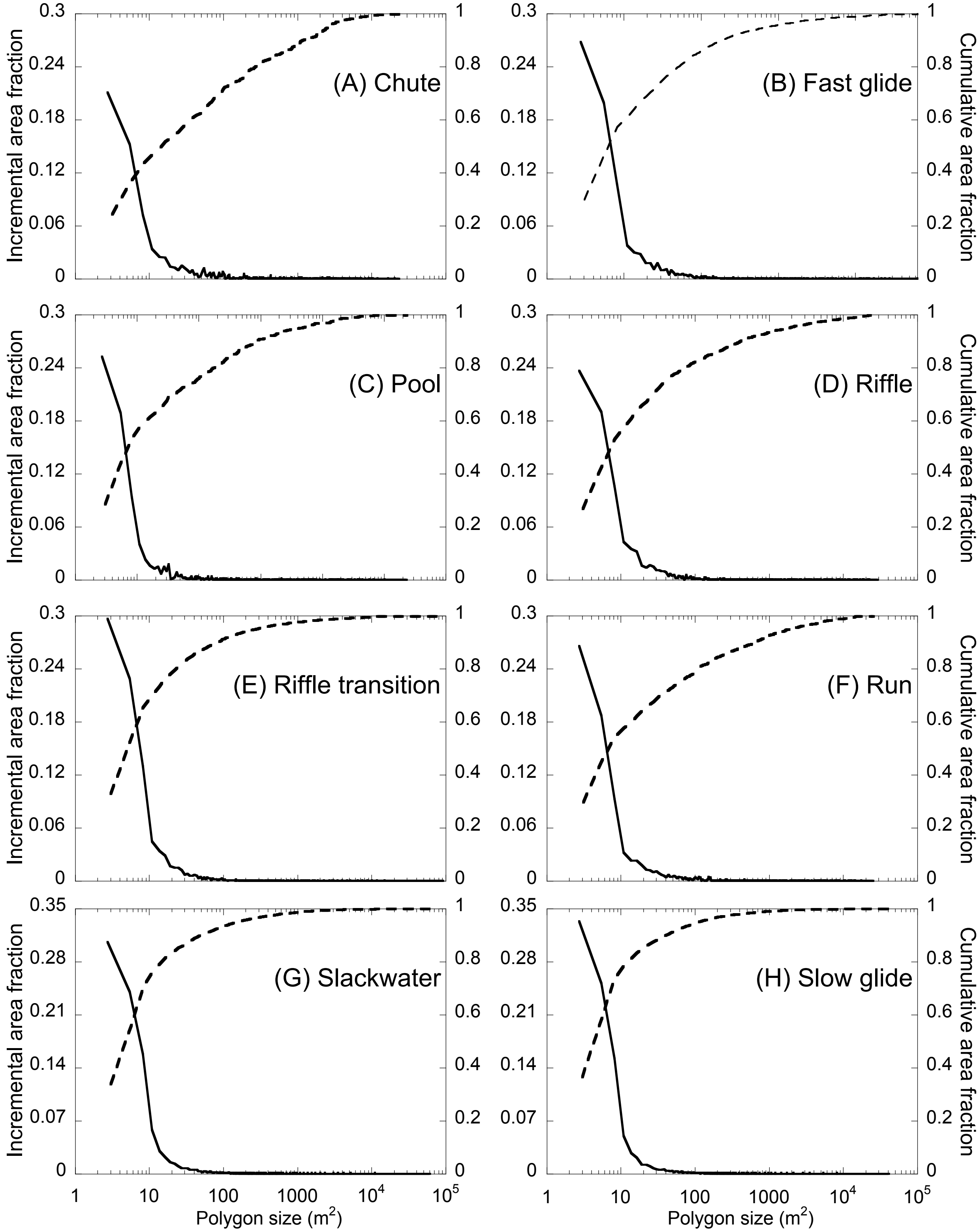

(A) Chute
(B) Fast glide
(C) Pool
(D) Riffle
(E) Riffle transition
(F) Run
(G) Slackwater
(H) Slow glide
Incremental area fraction
Cumulative area fraction
Polygon size (m^2)

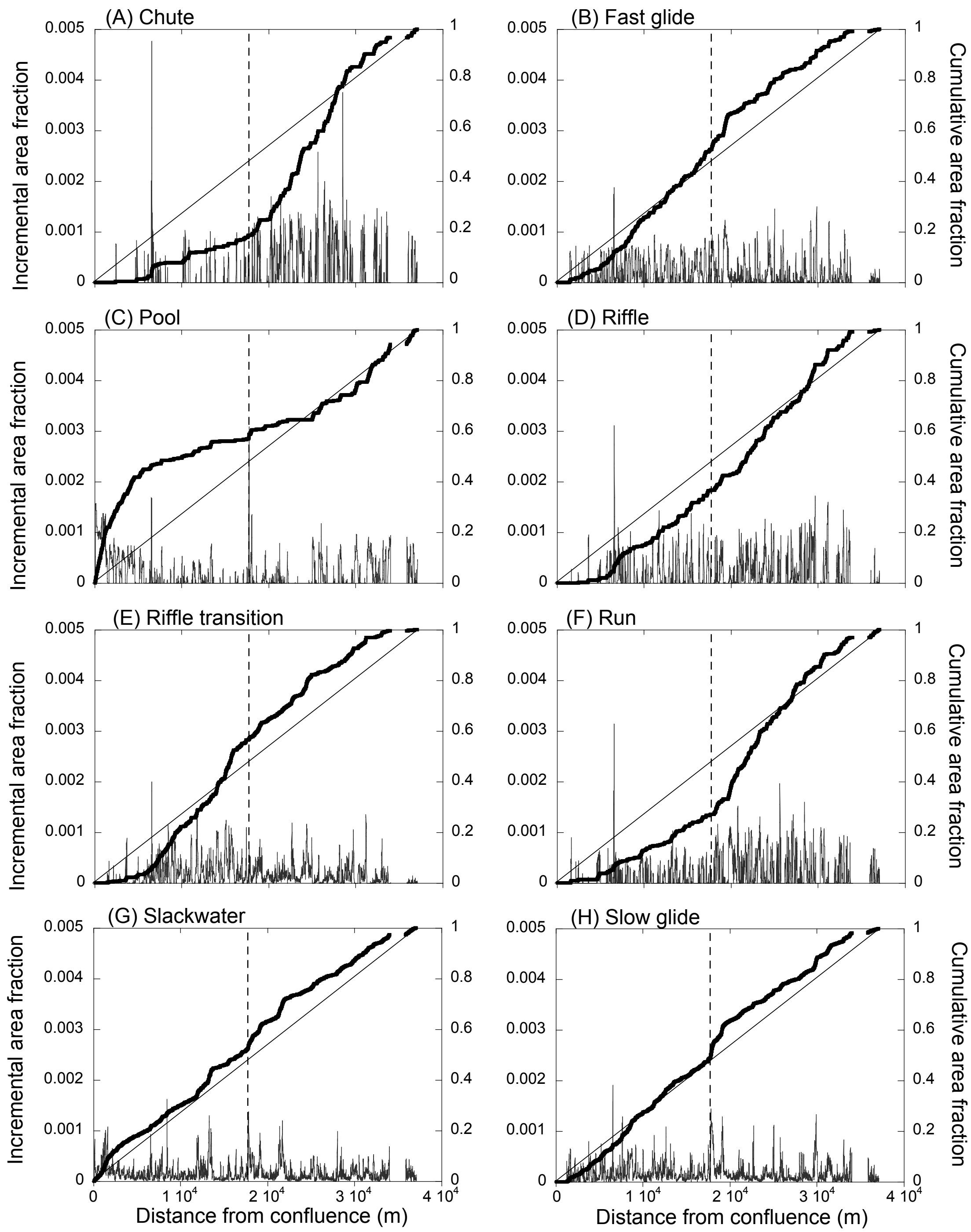
(A) Chute
(B) Fast glide
(C) Pool
(D) Riffle
(E) Riffle transition
(F) Run
(G) Slackwater
(H) Slow glide
Incremental area fraction
Cumulative area fraction
Distance from confluence (m)
0
0.001
0.002
0.003
0.004
0.005
0.2
0.4
0.6
0.8
1
1 10^4
2 10^4
3 10^4
4 10^4

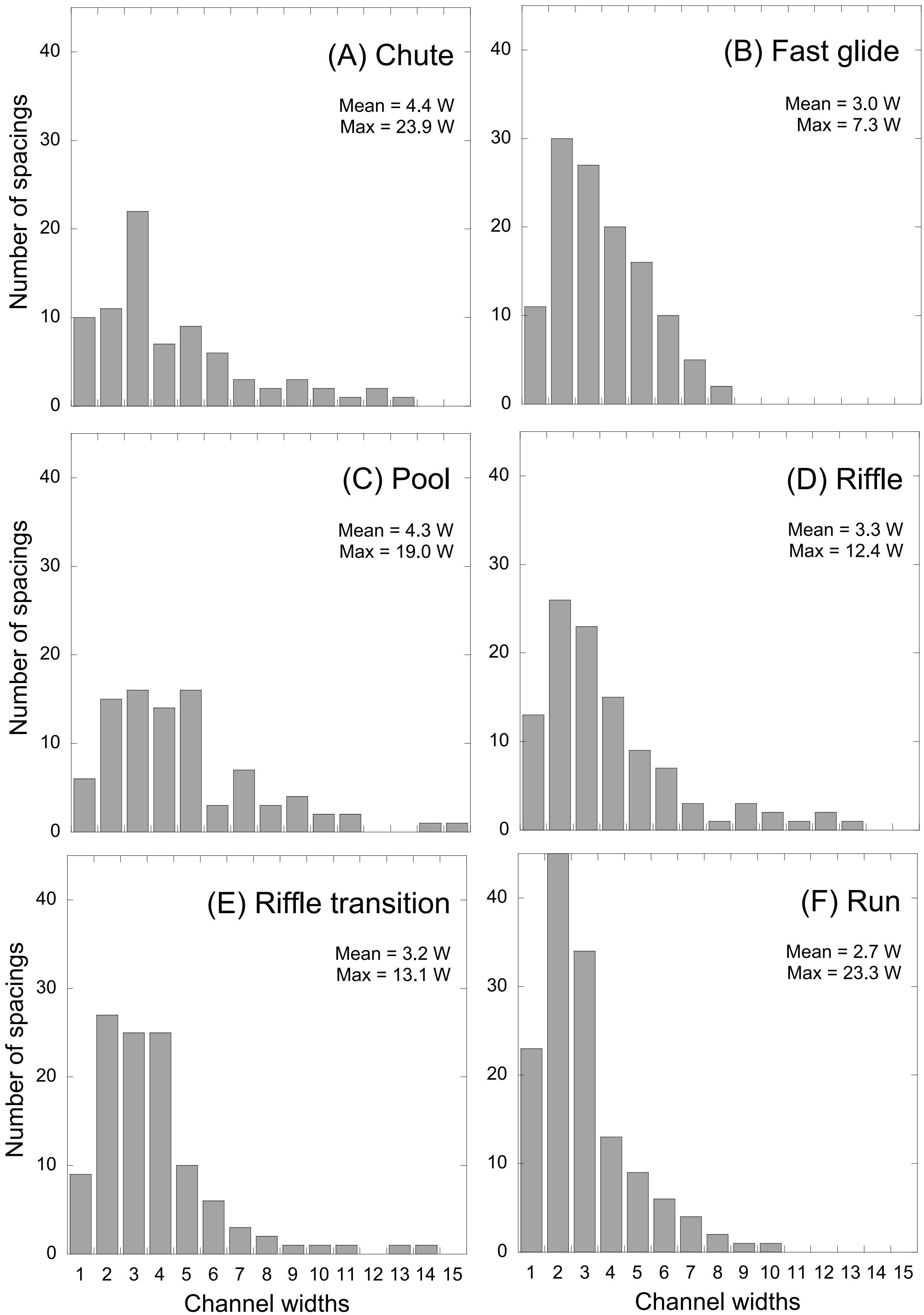
(A) Chute
Mean = 4.4 W
Max = 23.9 W
(B) Fast glide
Mean = 3.0 W
Max = 7.3 W
(C) Pool
Mean = 4.3 W
Max = 19.0 W
(D) Riffle
Mean = 3.3 W
Max = 12.4 W
(E) Riffle transition
Mean = 3.2 W
Max = 13.1 W
(F) Run
Mean = 2.7 W
Max = 23.3 W
Number of spacings
Channel widths
0
10
20
30
40
1 2 3 4 5 6 7 8 9 10 11 12 13 14 15

(A) All polygons

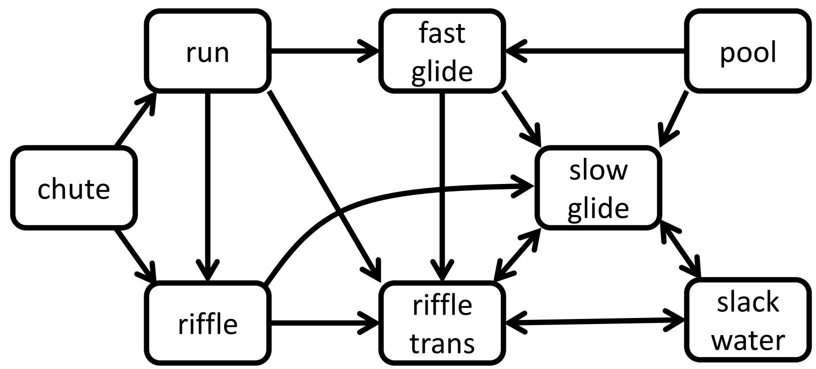

(B) Only polygons > 92.8 m^2

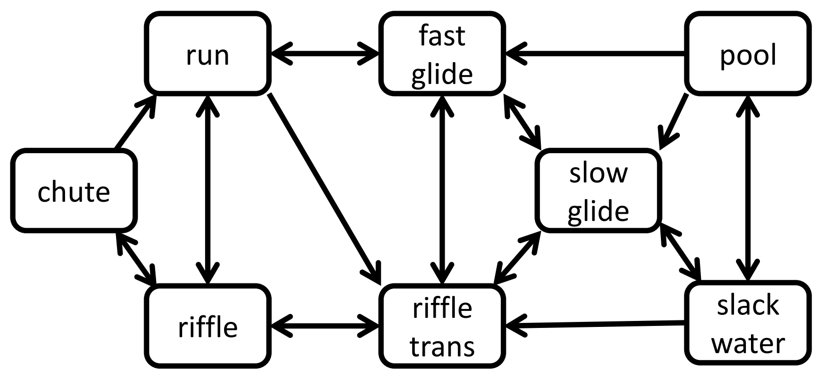

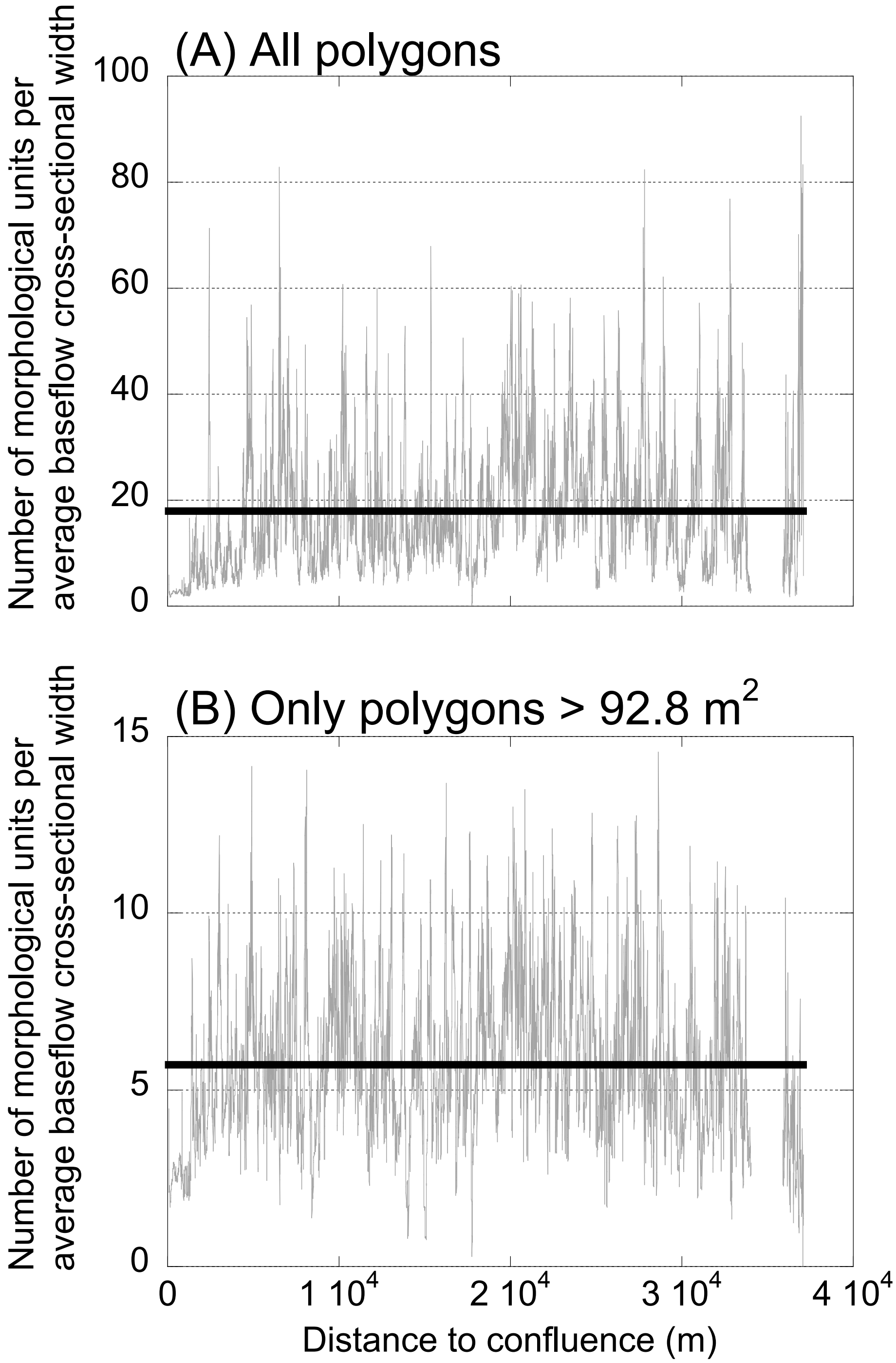

(A) All polygons
Number of morphological units per average baseflow cross-sectional width
100
80
60
40
20
0
(B) Only polygons > 92.8 m^2
Number of morphological units per average baseflow cross-sectional width
15
10
5
0
0
1 10^4
2 10^4
3 10^4
4 10^4
Distance to confluence (m)

LYR MU: areal divisions

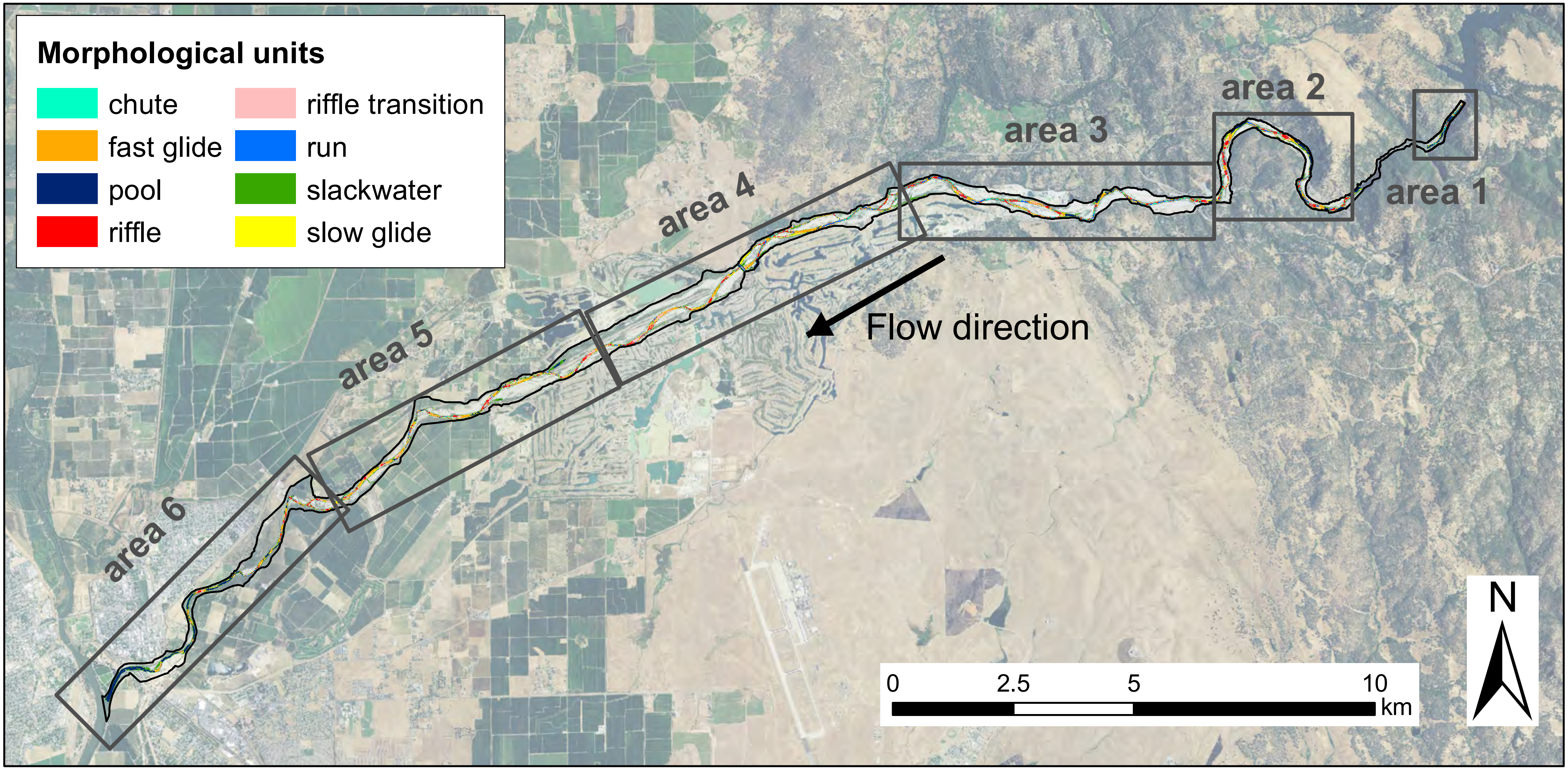

LYR MU: area 1

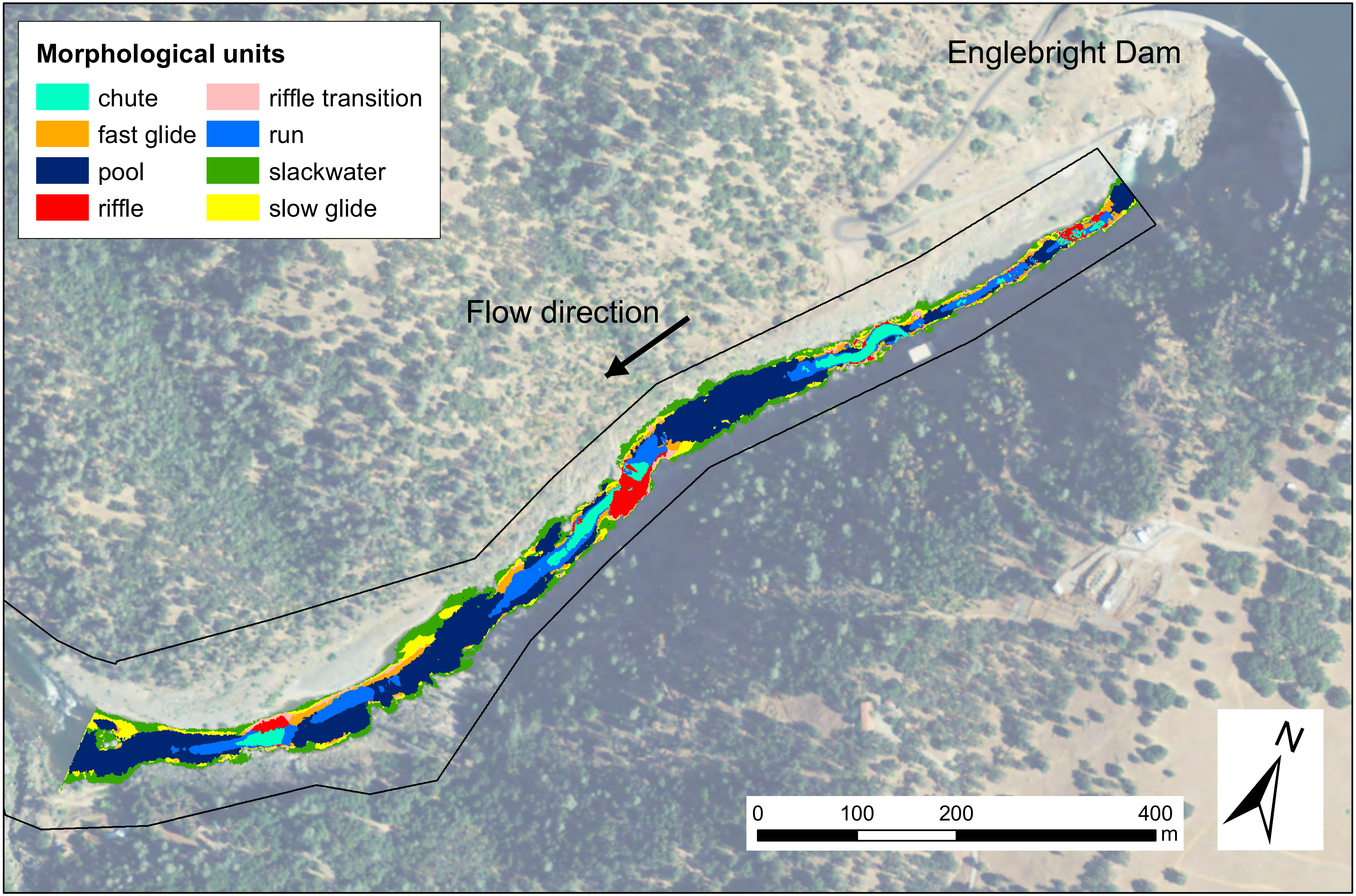

Morphological units
chute
fast glide
pool
riffle
riffle transition
run
slackwater
slow glide
Englebright Dam
Flow direction
0
100
200
400
m
N

LYR MU: area 2

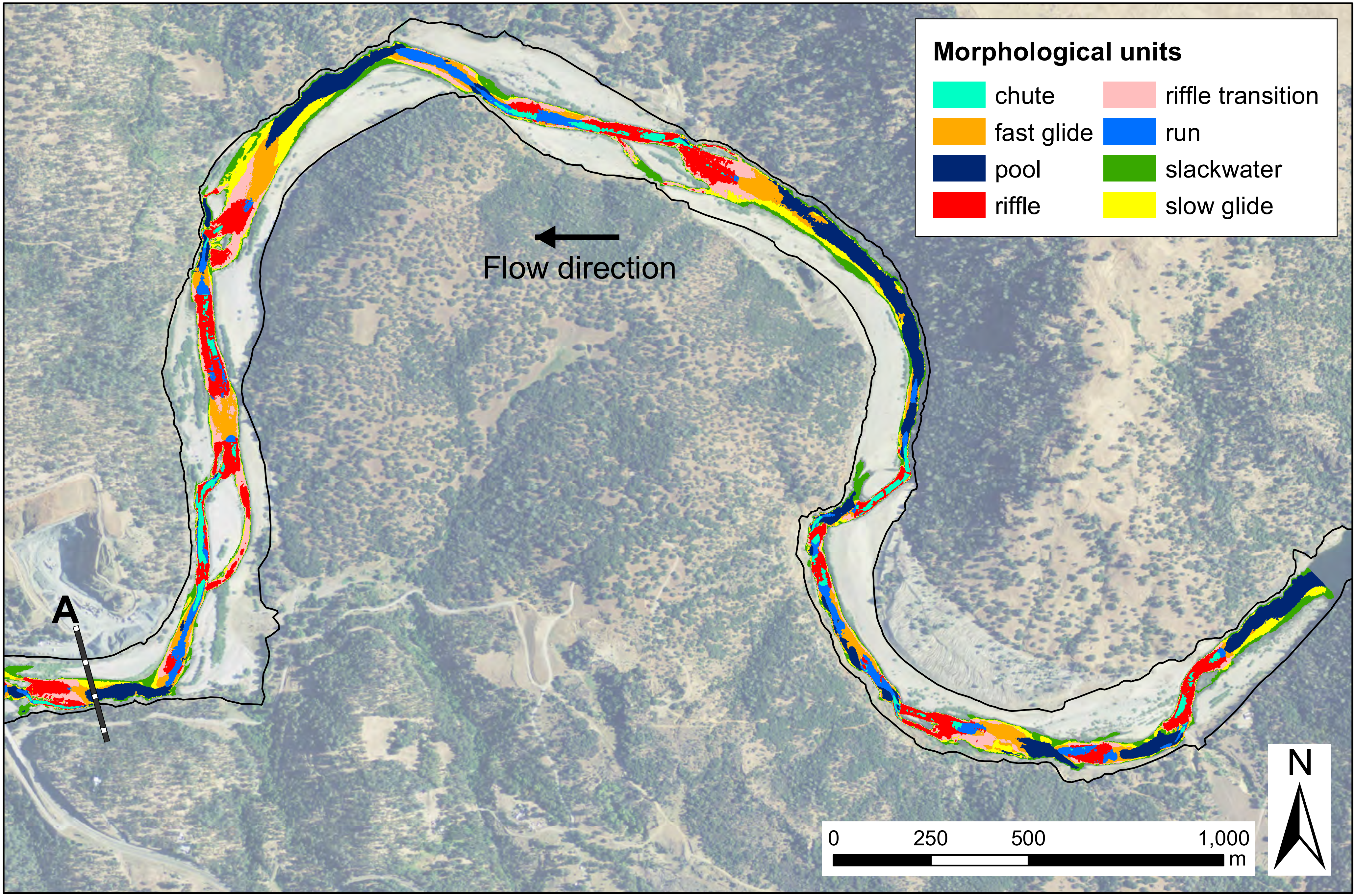

Morphological units
chute
fast glide
pool
riffle
riffle transition
run
slackwater
slow glide
Flow direction
A
N
0
250
500
1,000
m

LYR MU: area 3

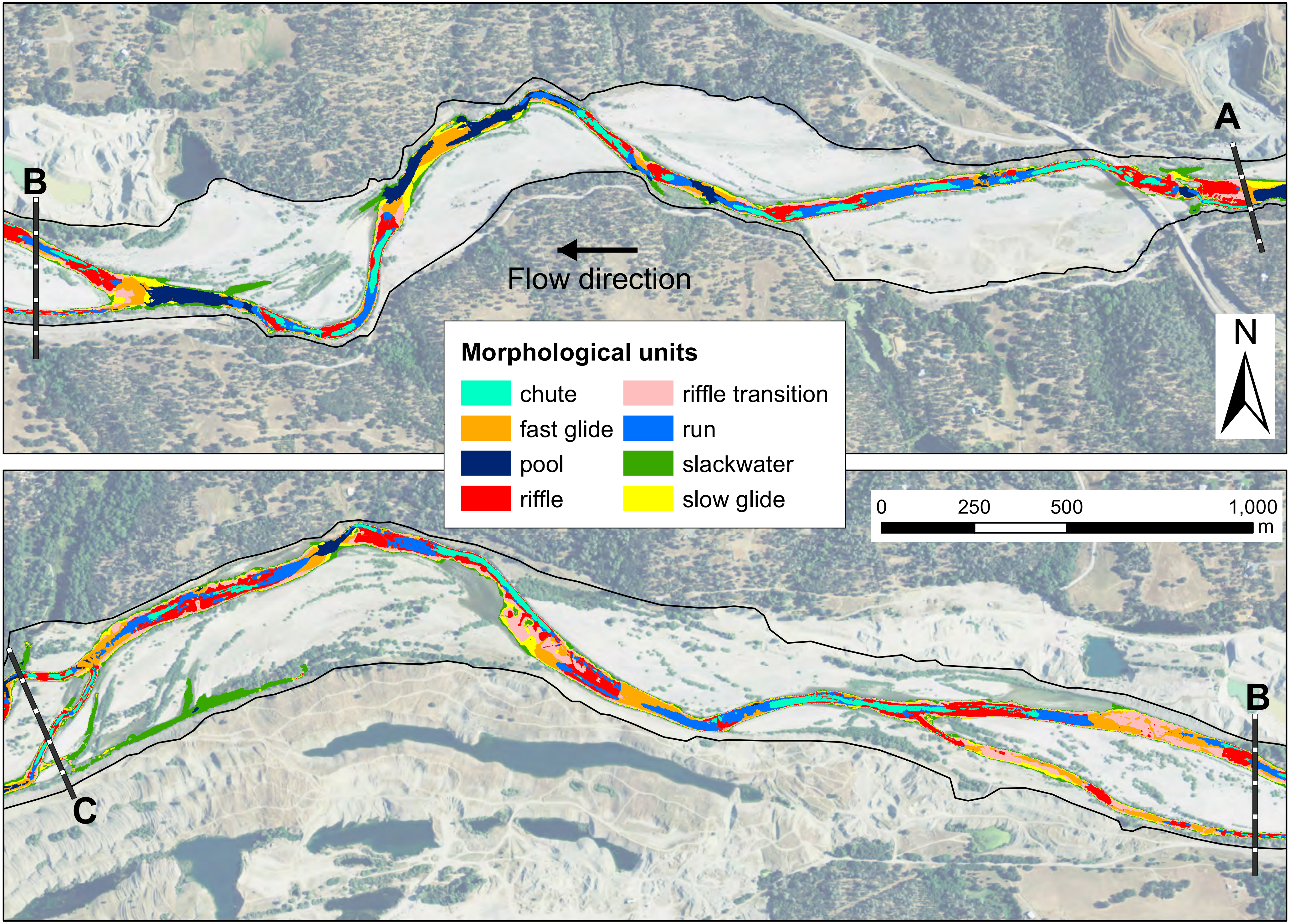
A
B
B
C
Flow direction
N
Morphological units
chute
fast glide
pool
riffle
riffle transition
run
slackwater
slow glide
0
250
500
1,000
m

LYR MU: area 4

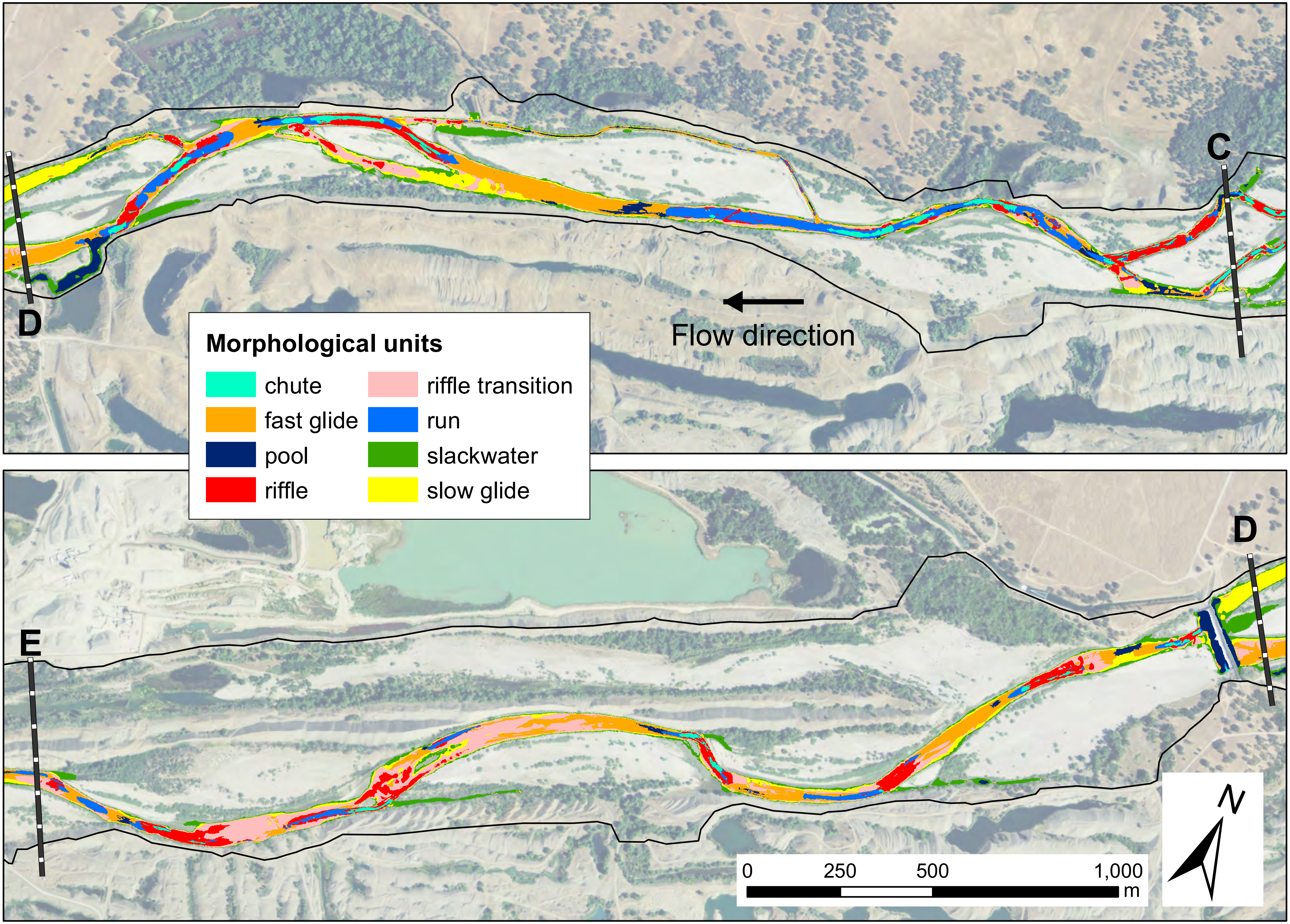

C
D
D
E
Flow direction
Morphological units
chute
fast glide
pool
riffle
riffle transition
run
slackwater
slow glide
0
250
500
1,000
m
N

LYR MU: area 5

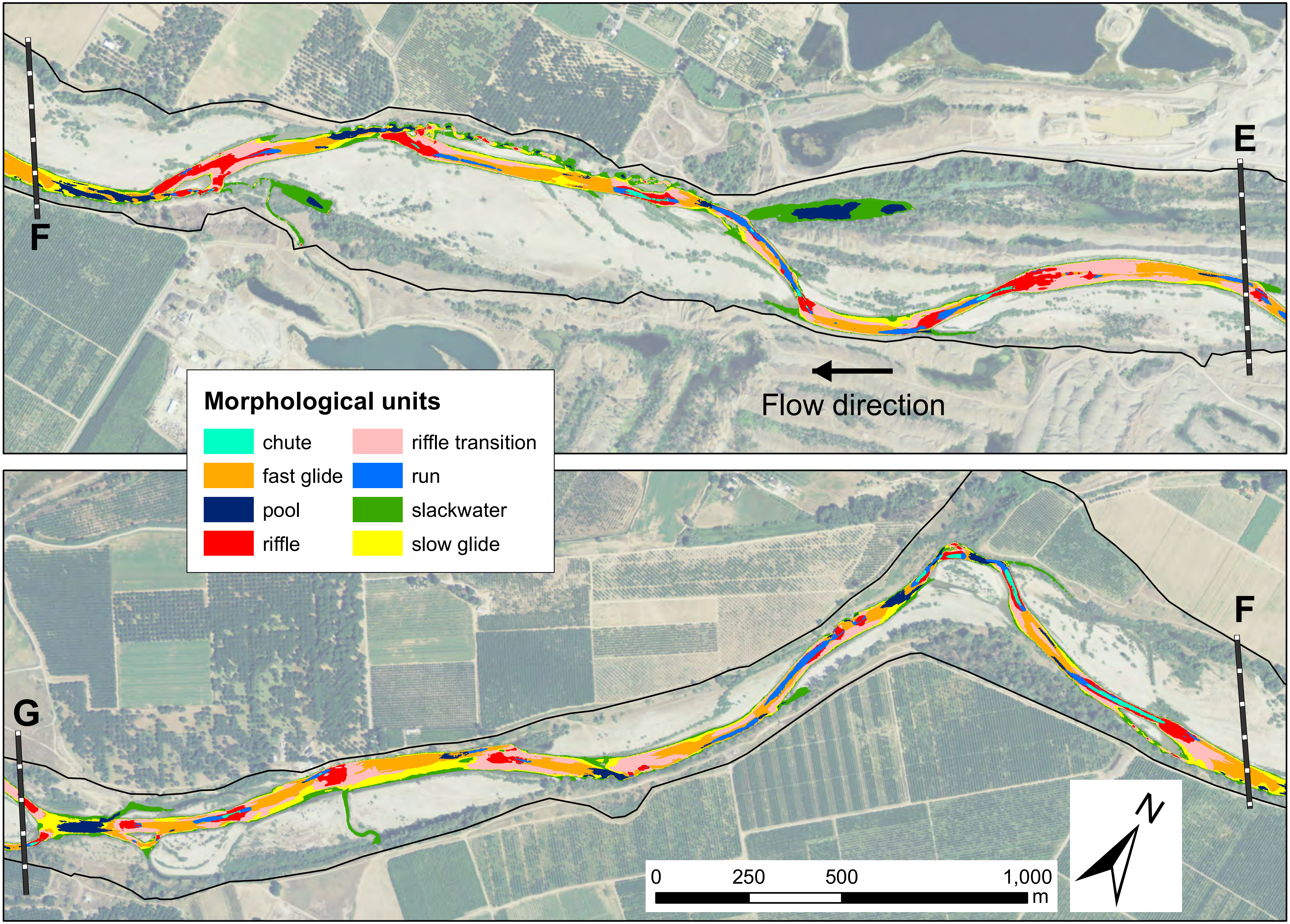
E
F
Flow direction
Morphological units
chute
fast glide
pool
riffle
riffle transition
run
slackwater
slow glide
G
F
0
250
500
1,000
m
N

LYR MU: area 6

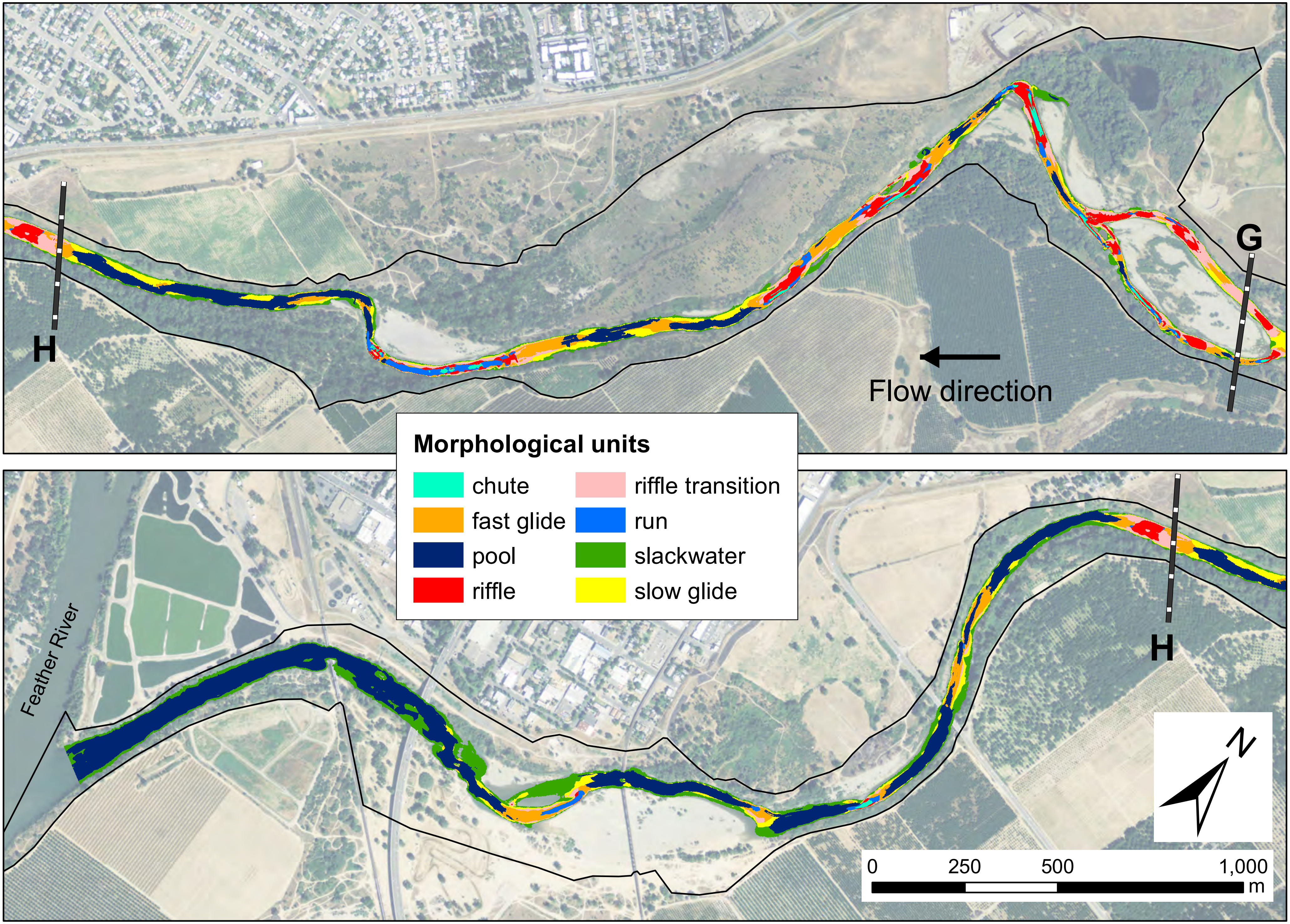

H
G
Flow direction
Morphological units
chute
fast glide
pool
riffle
riffle transition
run
slackwater
slow glide
H
Feather River
N
0
250
500
1,000
m